Effect of Particle Morphology on Strength of Glass Sands

Yang Xiao, M.ASCE[1]; Qingyun Fang[2]; Armin W. Stuedlein, M.ASCE[3]; and T. Matthew Evans, M.ASCE[4]

Abstract: A series of drained triaxial tests were performed on sandy soils [crushed glass (CG) and glass bead (GB)] with different mean particle sizes in order to investigate the effect of both particle size and particle shape on the soil strength and dilatancy. Four groups of angular CG sands with mean particle sizes of 0.227 to 1.001 mm, four groups of rounded GB sands with mean particle sizes of 0.374 to 0.836 mm, and one special group of subrounded GB sands with a mean particle size of 0.181 mm were tested at the same initial relative density of 60%. It was observed that, as the mean particle size increased for a similar particle shape, both the maximum and critical-state friction angles of the rounded GB sands increased, albeit marginally, whereas the critical-state friction angle of the angular CG sands showed a decrease. The maximum dilation angle of both the angular CG and rounded GB sands increased with an increase in the mean particle size. In addition, a Bolton's stress–dilatancy equation for glass sands was examined; the slope was found to be constant while the intercept varied slightly with different mean particle size. A comparison of the test results for the angular CG, rounded GB, and subrounded GB sands clearly demonstrated that the strength and friction angle of granular soils results directly from increased angularity where interparticle locking plays a crucial role.
DOI: 10.1061/IJGNAI.GMENG-8661.

Introduction

The shear strength and dilation of sandy soils are affected by their confining pressure and density (Charles and Watts 1980; Fukushima and Tatsuoka 1984; Been and Jefferies 1985; Kolymbas and Wu 1990; Chu 1995; Wan and Guo 1998, 1999; Li and Dafalias 2000; Lancelot et al. 2006; Varadarajan et al. 2006; Chakraborty and Salgado 2010; Cinicioglu and Abadkon 2015; Chen and Zhang 2016b; Esposito and Andrus 2017; Giampa and Bradshaw 2018), particle size and gradation (Al-Hussaini 1983; Muir Wood and Maeda 2008; Vangla and Latha 2015; Amirpour Harehdasht et al. 2017; Yang and Luo 2018; Deng et al. 2021), the addition of fines to the sand matrix (Salgado et al. 2000; Ni et al. 2004; Yang et al. 2006; Murthy et al. 2007; Carraro et al. 2009; Rahman et al. 2011; Yang and Wei 2012; Rahman and Lo 2014; Wei and Yang 2014; Chen and Zhang 2016a; Ng et al. 2017; Xiao et al. 2017a, 2017b; Hassan et al. 2022; Yilmaz et al. 2023), the addition of coarse aggregates to the soil mixture (Simoni and Houlsby 2006; Li 2013; Li et al. 2013; Wei et al. 2018; Shi et al. 2021), the addition of biotreated bonds (Wu et al. 2021a; Xiao et al. 2021b, 2022a, 2023a; Wu et al. 2023), particle shape (Cho et al. 2006; Yang and Wei 2012; Li et al. 2013; Wei and Yang 2014; Altuhafi et al. 2016; Gong and Liu 2017; Kandasami and Murthy 2017; Keramatikerman and Chegenizadeh 2017; Zhao and Zhou 2017; Alshibli and Cil 2018; Jiang et al. 2018; Zhou et al. 2018; Gong et al. 2019; Guida et al. 2019; Xiao et al. 2019a, b; Chen et al. 2021; Liang et al. 2022; Wang et al. 2022), interparticle friction, particle roughness (Cavarretta et al. 2010; Koval et al. 2011; Dai et al. 2016; Alshibli et al. 2017; Wu et al. 2017; Tovar-Valencia Ruben et al. 2018; Guida et al. 2019; Thakur Mohmad and Penumadu 2021), particle breakage (Muir Wood and Maeda 2008; Yao et al. 2008; Daouadji and Hicher 2010; Bandini and Coop 2011; Alikarami et al. 2015; Liu et al. 2017; Xiao and Liu 2017; Karatza et al. 2018; Yu 2019; Ciantia and O'Sullivan 2020; Zhang and Luo 2020; Xiao et al. 2022b, 2022c, 2023b), loading mode (i.e., load-controlled shearing for prefailure instability and deformation-controlled shearing for prefailure strain softening) (Chu et al. 1993; Chu and Leong 2001; Chu and Wanatowski 2009), stress and/or strain path (Tatsuoka et al. 1986; Lam and Tatsuoka 1988; Chu et al. 1992, 1993; Hanna 2001; Alshibli et al. 2003; Wanatowski and Chu 2007; Chu and Wanatowski 2008; Arda and Cinicioglu 2021; Shi et al. 2022), and drainage conditions (Chu and Lo 1994; Yamamoto et al. 2009; Chu et al. 2012; Zeybek and Madabhushi 2019).

Substantial observations and governing relationships have resulted from these and other studies that have identified the effects of particle size and shape on sediment strength and dilatancy. The role of increased angularity on the enhanced strength of granular materials represents one such finding (Hanna 2001; Amirpour Harehdasht et al. 2017; Suh et al. 2017; Alshibli and Cil 2018; Sarkar et al. 2019; Lashkari et al. 2020; Nguyen et al. 2020; Arda and Cinicioglu 2021; Deng et al. 2021; Shi et al. 2021; Wang et al. 2021; Wu et al. 2021b; Xiao et al. 2021a; Nie et al. 2022). For example, Guo and Su (2007) tested Ottawa sand, with rounded grains, and crushed limestone, with angular grains, and reported that angularity resulted in having a substantial effect on both the maximum friction angle (ϕ'_{max}) and the friction angle at the onset of dilation (ϕ'_f) as a result of improved interparticle locking. Yang and Wei (2012) observed, from a series of undrained triaxial tests on four binary mixtures of uniform (Toyoura and Fujian) sands with nonplastic fines (angular crushed silica fines and rounded glass beads), that the addition of the crushed silica fines increased

[1]Professor, Key Laboratory of New Technology for Construction of Cities in Mountain Area, State Key Laboratory of Coal Mine Disaster Dynamics and Control, School of Civil Engineering, Chongqing Univ., Chongqing 400045, China (corresponding author). ORCID: https://orcid.org/0000-0002-9411-4660. Email: hhuxyanson@163.com

[2]Graduated Student, School of Civil Engineering, Chongqing Univ., Chongqing 400045, China. Email: fqy_cqu@163.com

[3]Professor, School of Civil and Construction Engineering, Oregon State Univ., Corvallis, OR 97331. ORCID: https://orcid.org/0000-0002-6265-9906. Email: Armin.Stuedlein@oregonstate.edu

[4]Professor, School of Civil and Construction Engineering, Oregon State Univ., Corvallis, OR 97331. ORCID: https://orcid.org/0000-0002-8457-7602. Email: matt.evans@oregonstate.edu

Note. This manuscript was submitted on November 28, 2022; approved on March 7, 2023; published online on May 22, 2023. Discussion period open until October 22, 2023; separate discussions must be submitted for individual papers. This paper is part of the ***International Journal of Geomechanics***, © ASCE, ISSN 1532-3641.

the critical-state friction angle (ϕ'_{cs}). Contrastingly, the addition of the glass beads decreased the ϕ'_{cs} of the binary mixtures because the particles of the crushed silica fines were more angular than the particles of the Toyoura and Fujian sands, whereas the glass beads were more rounded than those of the host sands. These findings were explained by a proposed particle-scale conceptual model, wherein the interparticle contacts, movements, and rearrangements became more difficult when the particles of the fines and host sands were more angular because these binary particles made a more stable structure. The drained and undrained shear test results for mixtures of the host sands investigated by Yang and Luo (2015) showed that an increase in overall regularity (defined in the next section) led to a decrease in ϕ'_{cs}. Xiao et al. (2019a) described drained triaxial test experiments on glass sands with varying mixtures of angular and rounded particles, concluded that both the $\phi'_{\max}$ and ϕ'_{cs} increased with increasing angularity, but the maximum dilatancy angle ($\psi_{\max}$) increased with decreasing angularity. They proposed a stress–dilatancy equation that considered the effect of overall regularity. The phenomenon of the effect of particle shape on the $\phi'_{\max}$, ϕ'_{cs}, and $\psi_{\max}$ observed by Xiao et al. (2019a) was verified by Thakur Mohmad and Penumadu (2021), who pointed out that particle shape rather than interparticle friction determined the localized deformation. Meanwhile, Zhang et al. (2020) also found that an increase in roundness resulted in an increase in the $\psi_{\max}$. The effect of particle shape on the $\psi_{\max}$, and its contribution to the strength, depends on density. For example, Shi et al. (2021) found that the critical-state shear strength of gap-graded soils in a dense state increased continuously with an increase in the fraction of subangular feldspar gravel, while the addition of rounded steel beads at a volume fraction of 0% to 44.5%, or the addition of subangular gravel at a volume fraction of 0% to 32.2%, did not change the shear strength of the gap-graded soils in a loose state. They argued that the extra strength could be attributed to the force transmission of densified sand bridges forming between the coarse aggregates. Furthermore, drained tests reported by Yilmaz et al. (2023) determined that the addition of more-angular and finer particles to angular coarse sands (where the fines content was within the threshold value for a sand matrix) resulted in a decrease in the $\phi'_{\max}$ and $\psi_{\max}$. These results do not agree with the findings of Yang and Wei (2012), however. In explaining this discrepancy, Yilmaz et al. (2023) pointed to the particle-column mechanism proposed by Oda (1972) and Iwashita and Oda (2000), where the finer particles fill the void between neighboring columns, providing lateral support to the particle columns, and suppressing buckling and dilation, resulting in a decrease in the $\phi'_{\max}$ and $\psi_{\max}$. By contrast, Yang and Wei (2012) proposed a particle-scale model in which the addition of finer angular grains made the mixture more stable. These different findings may have arisen from variations in the density, pressure, and/or particle shape of the tested soils.

The effect of particle size on the friction angle has been subject to much debate. One viewpoint is that the shear strength decreases with increasing particle size (Marschi et al. 1972; Ovalle et al. 2014; Ovalle and Dano 2020). Marschi et al. (1972) conducted drained triaxial tests on angular rockfill materials with a range of parallel gradings, showing that the internal friction angle decreased with an increase in the particle size, which was adopted in the size-effect relation theory proposed by Frossard et al. (2012) and confirmed by Ovalle et al. (2014) and Ovalle and Dano (2020) with their test results. Also, Amirpour Harehdasht et al. (2017) performed a series of drained triaxial tests on both rounded glass beads and subrounded and subangular Péribonka sand, and found that the $\phi'_{\max}$ and $\psi_{\max}$ of the two materials decreased with an increase in particle size. In addition, a series of direct shear tests on rounded basalt microspheres, subangular and angular Eastmain sand, and subrounded and subangular Péribonka sand, conducted by Amirpour Harehdasht et al. (2019), showed that an increase in particle size led to a decrease in the shear strength and dilation. Another viewpoint is that the shear strength increases with increasing particle size (Bagherzadeh-Khalkhali and Mirghasemi 2009; Hamidi et al. 2012). Bagherzadeh-Khalkhali and Mirghasemi (2009) and Hamidi et al. (2012) both found that the peak-state shear strength and dilation of Tehran coarse-grained soils increased with increasing maximum particle size for both parallel and increasingly better-graded gradations. Dai et al. (2016) performed a series of direct shear tests on glass beads, determining that both the $\phi'_{\max}$ and ϕ'_{cs} increased with increasing mean particle size, and that glass sands with a larger particle size exhibited a more dilative shear response. Recent work by Ari and Akbulut (2022) revealed that the $\phi'_{\max}$, $\psi_{\max}$, and repose angle (ϕ'_a) of angular sands increased with an increase in the mean particle size, which contradicts these prior findings (Marschi et al. 1972; Ovalle et al. 2014; Amirpour Harehdasht et al. 2017, 2019; Ovalle and Dano 2020). A third viewpoint is that the change in shear strength with particle size depends on particle shape in granular soils (Varadarajan et al. 2003; Honkanadavar and Sharma 2016). Varadarajan et al. (2003) reported triaxial test results for two rockfill materials representing rounded/subrounded and angular/subangular particle shapes, discovering that the friction angle increased with increasing particle size for the rounded/subrounded materials, whereas the friction angle decreased with increasing particle size for the angular/subangular materials. These findings have been further verified by other test data (Varadarajan et al. 2006; Honkanadavar and Sharma 2014, 2016), implying that the effect of particle shape cannot be ignored in some cases when exploring the effect of particle size on shear strength and dilation in granular materials. For granular soils with angular particles, this viewpoint is partially in line with the first viewpoint, and for granular soils with rounded particles, it also partially agrees with the second viewpoint. The last viewpoint is that the change in shear strength with particle size is marginal. Discrete-element method (DEM) simulations on initially nonoverlapping two-dimensional (2D) rounded discs, as reported by Sitharam and Nimbkar (2000), demonstrated that an increase in particle size leads to a marginal increase (or no increase) in the internal friction angle at any given confining pressure. Vangla and Latha (2015) also pointed out that the $\phi'_{\max}$ of angular sands with similar particle shape and void ratio was unaffected by particle size, although the ultimate friction angle (ϕ'_r) and ϕ'_a increased with an increase in particle size. Recently, Deng et al. (2021) conducted a series of drained triaxial shear tests on subangular Pasabahce silica sand, confirming the first viewpoint that an increase in particle size leads to a decrease in the $\phi'_{\max}$ and $\psi_{\max}$, similar to the trend for subangular Péribonka sand, as investigated by Amirpour Harehdasht et al. (2017), although with ϕ'_{cs} decreasing with an increase in particle size because particle size in their work was not isolated from other factors (e.g., particle shape or roughness) that could have affected the $\phi'_{\max}$, $\psi_{\max}$, and ϕ'_{cs}, and the stress–dilatancy relationship. It is clear that there remains a lack of consensus as to the role of particle size due to the confounding influence of particle shape, roughness, grading, etc., which may have been overlooked in the studies reviewed in the preceding discussion. It was therefore critical to evaluate the effect of particle size considering highly controlled materials that possessed the same particle shape and gradation—the latter, for example, through the coefficient of uniformity, C_u. This work presents the results of an experimental program conducted on glass sands to isolate the effects of particle size and particle shape, quantified using the mean particle size, D_{50}, and overall

regularity, respectively, on the strength and dilatancy of granular materials.

Experimental Program and Materials

The experimental program described in this study consists of tests on glass sands, including crushed glass (CG) and glass bead (GB) sands, supplied by the Zhaotong Glass & Plastic Technology Company (Guangdong Province, China). The mineral comprising these glass sands is mainly silicon dioxide, and the specific gravity and Mohs hardness are 2.45 and 6, respectively. Four groups of CG sands with $D_{50} \in [1.001, 0.782, 0.388, 0.227]$ mm, and five groups of GB sands with $D_{50} \in [0.836, 0.747, 0.561, 0.374, 0.181]$ mm were prepared through sieving. The gradation in the four groups of CG sands was similar, with an average C_u of 1.6, and with the five groups of GB sands also possessing the same gradation, with an average C_u of 1.1. Figs. 1(a and b) illustrate the particle size distributions of the CG and GB sands in terms of the minimum Feret diameter, as recommended by Altuhafi et al. (2013). Figs. 1(c–f) present the variations in three shape parameters, including the aspect ratio (A_R), convexity (C_X), and sphericity (S_C) of particles with different values of D_{50}. Note that A_R is expressed as the ratio of the minimum Feret diameter ($D^F_{\min}$) to the maximum Feret diameter ($D^F_{\max}$)—that is, $A_R = D^F_{\min}/D^F_{\max}$; C_X is defined as the ratio of the projection area (A) and the area of the convex hull ($A+B$), formulated as $C_X = A/(A+B)$; and S_C is the ratio of the perimeter of the equivalent circle (P_{eq}) to the real perimeter (P_r), formulated as $S_C = P_{eq}/P_r$. The values of A_R, C_X, and S_C for all nine glass sands were evaluated as those corresponding to 50% of the accumulative distribution of the particle shape, as shown in Figs. 1(c–f). The overall regularity (O_R) proposed by Yang and Luo (2015) for the comprehensive assessment of particle shape was adopted in this study, where $O_R = (A_R + C_X + S_C)/3$. The values of O_R were 0.782, 0.779, 0.781, and 0.781 corresponding to $D_{50} = 1.001$, 0.782, 0.388, and 0.227 mm for the CG sands, and 0.935, 0.935, 0.934, 0.929, and 0.911 corresponding to $D_{50} = 0.836$, 0.747, 0.561, 0.374, and 0.181 mm for the GB sands. As shown in Figs. 1(e and f), the distributions of A_R and C_X in the subrounded GB sands with $D_{50} = 0.181$ mm are significantly broader than those of other rounded GB sands, indicating the presence of oblong particles, resulting from manufacturing-induced imperfections, including the bonding of small beads to larger beads. The remaining four rounded glass sands, each with similar C_u, A_R, C_X, S_C, and O_R, were investigated to obtain an appropriate assessment of the effect of particle size on the strength and dilatancy of the

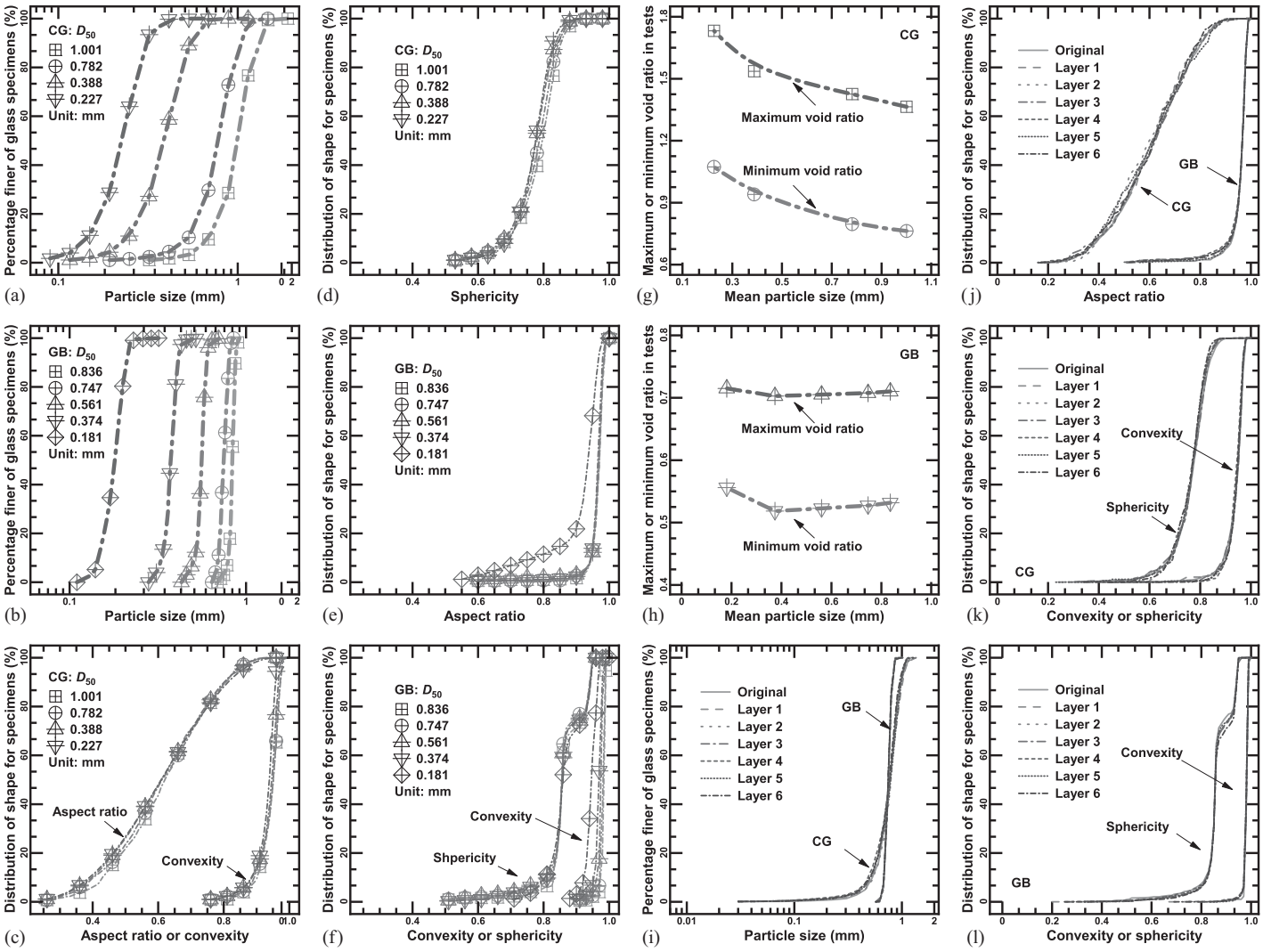

Fig. 1. Basic properties of CG and GB sands: (a and b) particle size distribution; (c–f) distribution of particle shape parameters; (g and h) variations in maximum and minimum void ratios; and (i–l) differences in particle characteristics with specimen height after testing.

sands in the absence of other contributing variables, such as particle gradation and shape, which also applies to the other four angular glass sands. The maximum, e_{max}, and minimum, e_{min}, void ratios of these materials were determined in accordance with ASTM standards (ASTM 2016a, b). As shown in Figs. 1(g and h), the e_{max} and e_{min} of the CG sands decreased with increasing particle size, similar to the observations reported by Miura et al. (1998) and Cubrinovski and Ishihara (2002). It was noted that the e_{max} and e_{min} of the GB sands exhibited little sensitivity to particle size, as has also been observed by other researchers (Graton and Fraser 1935; Lade et al. 1998). Furthermore, the e_{max} and e_{min} increased with increasing angularity, consistent with the tendencies reported by Cho et al. (2006) and Xiao et al. (2019a). All particle size distribution and particle shape parameter measurements were performed using a Quick-Picture (QICPIC) instrument (Sympatec, Clausthal-Zellerfeld, Germany). A series of strain-controlled, consolidated, drained triaxial tests were performed using a triaxial apparatus (Global Digital Systems, Ltd., Hook, UK). All specimens with a diameter of 39.1 mm and a height of 80 mm were prepared to achieve an initial relative density of 60% using the moist tamping undercompaction method (Ladd 1978), with de-aired water at a 5% water content (by weight) and compacted in the mold using six layers. Once the top cap was placed on the specimen, the mold was removed using a vacuum of 10 kPa applied to the sample. Then, the specimen was placed in a triaxial cell that was filled with de-aired water, and was later saturated at a 20 kPa effective confining stress, equal to the difference between the cell pressure and the back pressure, which were raised in uniform increments until the measured B-value was greater than or equal to 0.98. Thereafter, the sample was subjected to a given effective consolidation pressure (e.g., $\sigma'_{3c} = 0.05$, 0.1, 0.2, and 0.4 MPa) and was sheared at a rate of vertical displacement of 0.18 mm/min. Given that specimen uniformity and particle breakage following shear can influence the interpretation of the test results (Indraratna et al. 1998; Tarantino and Hyde 2005), the effect of specimen uniformity was investigated, following the previous studies of Zhang et al. (2018) and Xiao et al. (2019a). Figs. 1(i–l) present the cumulative distributions of the particle size and particle shape parameters derived from the six lifts (i.e., Layers 1–6, from the top to the bottom of the specimens) before and after the triaxial tests, including specimens of the angular CG sands with $D_{50} = 0.782$ mm and the rounded GB sands with $D_{50} = 0.747$ mm, tested at $\sigma'_{3c} = 0.4$ MPa. The postshear cumulative distributions of particle size—A_R, C_X, and S_C—for each compaction lift were nearly identical to the preshear cumulative distributions, indicating uniformity of the specimen and a lack of particle breakage during shear.

Test Results on Stress–Strain Relationship

Figs. 2(a–p) present the stress–strain relationships of the angular CG and rounded GB sands with a given D_{50} at $\sigma'_{3c} = 0.05$, 0.1, 0.2, and 0.4 MPa. The deviatoric stress, stress ratio, axial strain, and volumetric strain are denoted as q, η, ε_a, and ε_v, respectively. All of the angular CG and rounded GB sands in the initially medium-dense state exhibited strain softening to some degree. For the angular CG sands with different values of D_{50}, Figs. 2(a–d) show that an increase in σ'_{3c} at a given ε_a resulted in an increase in q. The axial strain (ε^a_{max}) corresponding to the maximum deviatoric stress (q_{max}) increased with an increase in σ'_{3c}, which can also be clearly observed in Figs. 2(e–h), where the ε_a corresponding to the q_{max} was identical to that corresponding to the maximum stress ratio (η_{max}). Also, Figs. 2(e–h) show that the η_{max} of the angular CG sand specimens increased with a decrease in σ'_{3c}. These observations are consistent with the typical stress–dilatancy characteristics observed in natural sands (Salgado et al. 2000; Guo and Su 2007; Deng et al. 2021).,The rounded GB sands at a higher σ'_{3c}, as shown in Figs. 2(i–l), exhibited more strain softening than the angular CG sands, although the rounded GB sands possessed the same behavior with the variation in q with σ'_{3c} at a given ε_a. It was also noted that the η_{max} slightly increased with increasing σ'_{3c} in the rounded GB sands, as shown in Figs. 2(m–p), which is opposite to the angular CG sands, as shown in Figs. 2(e–h). For example, an increase in σ'_{3c} from 0.05 to 0.4 MPa in the angular CG sands with $D_{50} = 1.001$ mm led to a decline in the η_{max}, from 1.86 to 1.54, whereas the comparable rounded GB sands with $D_{50} = 0.836$ mm resulted in a slight rise in the η_{max}, from 0.97 to 1.06, over the same range in σ'_{3c}. Also, the variation in ε^a_{max} with σ'_{3c} was marginal for the rounded GB sands, which was also different from the angular CG sands. It appears that the rounded GB sands were less sensitive to σ'_{3c}. Furthermore, the rounded GB sands exhibited stick–slip behavior during shear, as has previously been reported (Adjemian and Evesque 2004; Alshibli and Roussel 2006; Cui et al. 2017; Wu et al. 2017), which appears to have increased in amplitude with increasing σ'_{3c} [Figs. 2(i–l)]. For example, the maximum stick–slip reduction in deviatoric stress was 0.008, 0.016, 0.034, and 0.076 MPa for $\sigma'_{3c} = 0.05$, 0.1, 0.2, and 0.4 MPa, respectively, in the rounded GB sands with $D_{50} = 0.747$ mm. Figs. 3(a–p) show the stress–strain relation of the angular CG and rounded GB sands for different values of D_{50} at a given σ'_{3c}. An increase in D_{50} in the angular CG sands resulted in a minor increase in the q_{max} and η_{max} at a low value of σ'_{3c}, as presented in Figs. 3(a–h), with a minor, albeit opposite, trend at the high value of σ'_{3c}. For example, increasing the D_{50} of the angular CG sands from 0.227 to 1.001 mm at $\sigma'_{3c} = 0.05$ MPa led to a small increase in the q_{max}, from 0.231 to 0.245 MPa, and the η_{max}, from 1.82 to 1.86. At $\sigma'_{3c} = 0.4$ MPa, an increase in the D_{50} of the angular CG sands, from 0.227 to 1.001 mm, resulted in a small reduction in the q_{max}, from 1.32 to 1.27 MPa, and the η_{max}, from 1.57 to 1.54. By contrast, the rounded GB sands exhibited a consistent trend, where an increase in the D_{50} at a given σ'_{3c} resulted in a small increase in the q_{max}, η_{max}, and residual deviatoric stress, q_{rs} (corresponding to $\varepsilon_a \approx 30\%$), as shown in Figs. 3(i–p). For a given D_{50}, variations in ε_v with ε_a were compared for different values of σ'_{3c}, as shown in Figs. 4(a–d) for the angular CG sands and in Figs. 4(e–h) for the rounded GB sands, whereas the effect of D_{50} on the $\varepsilon_v - \varepsilon_a$ relationship at a given σ'_{3c} is presented in Figs. 4(i–l) for the angular CG sands and Figs. 4(m–p) for the rounded GB sands. The angular CG sands exhibited a notable suppression in dilation as σ'_{3c} increased, whereas the rounded GB sands appear to have been relatively insensitive to σ'_{3c} over its investigated range. Theses volume-change observations are consistent with the large difference in η_{max} observed for the angular CG sands for different values of σ'_{3c} in Figs. 2(e–h) and the small difference in η_{max} for the rounded GB sands in Figs. 2(m–p), as mentioned above. Furthermore, the difference in the $\varepsilon_v - \varepsilon_a$ relationship for different values of D_{50} was notable for the angular CG sands [Figs. 4(i–l)], whereas the difference was smaller for the rounded GB sands [Figs. 4(m–p)]. For example, the residual volumetric strain (ε^v_{rs}, corresponding to $\varepsilon_a \approx 30\%$) at $\sigma'_{3c} = 0.05$ MPa changed from −9.0% to −11.3% in the angular CG sands with an increase in D_{50} from 0.227 to 1.001 mm, and from −3.1% to −4.0% in the rounded GB sands with increasing D_{50} from 0.374 to 0.836 mm, respectively. The absolute values for the maximum difference in ε^v_{rs} were 2.3% for the angular CG sands at $\sigma'_{3c} = 0.05$ MPa, but only 0.9% for the rounded GB sands. These observations are similar for other magnitudes of σ'_{3c}.

Figs. 5(a–h) compare the stress–strain and volumetric responses of the angular CG and rounded GB sands with similar particle size

(e.g., the angular CG sands with $D_{50} = 0.782$ mm versus the rounded GB sands with $D_{50} = 0.747$ mm) that sheared at the same σ'_{3c} in order to demonstrate the isolated role of particle shape. The results clearly indicate that the improved particle interlocking associated with the highly angular CG sands served to dramatically increase the shear strength. For example, the values of q_{max} and q_{rs} at $\sigma'_{3c} = 0.4$ MPa were 1.289 and 1.155 MPa, respectively, for the angular CG sands, and these are much higher than those (i.e., 0.636 and 0.452 MPa, respectively) for the rounded GB sands. The highly angular CG sands exhibited twice the q_{max} of the rounded GB sands, while exhibiting significantly greater initial contraction and smaller dilation at $\sigma'_{3c} = 0.4$ MPa. The difference in the q_{max} between the angular CG and rounded GB sands with similar diameter at $\sigma'_{3c} = 0.05$ MPa was even greater (i.e., approximately 3.3 times higher) because the dilative response of the angular CG sands was not effectively suppressed under the low confining pressure. The test results for the angular CG sands with $D_{50} = 0.388$ mm and the rounded GB sands with $D_{50} = 0.374$ mm were plotted and are compared in Figs. 5(i–p), which shows the same trends in the responses of q_{max} and ε_v as those described for glass sands with larger diameters in Figs. 5(a–h). The angular CG sands exhibited greater dilation than the rounded GB sands at low σ'_{3c}, with greater suppression of dilation under higher confining pressures, while maintaining greater shear strength (e.g., $q_{max} = 0.232$ MPa for the angular CG sands vs. $q_{max} = 0.067$ MPa for the rounded GB sands at $\sigma'_{3c} = 0.05$ MPa; and $q_{max} = 1.323$ MPa for the angular CG sands vs. $q_{max} = 0.589$ MPa for the rounded GB sands at $\sigma'_{3c} = 0.4$ MPa). These results clearly point to the role of particle shape in enhancing particle interlocking despite the increased suppression of dilation under large values of σ'_{3c}. It can also be observed that the angular CG sands required a larger value of ε^a_{max} to reach the maximum shear resistance compared with the rounded GB sands for the same relative density and similar particle size. Furthermore, these angular particles exhibited reduced strain softening, confirming the observations of Guo and Su (2007). Figs. 5(i–p) also present the different mechanical responses exhibited by the rounded and subrounded GB sands with $D_{50} = 0.374$ and 0.181 mm, respectively. As mentioned previously, differences in the D_{50} led to only marginal changes in the shear strength and dilation, particularly when the difference in D_{50} was limited. The notable differences in the stress–strain and volumetric strain responses between the rounded and subrounded GB sands, with the

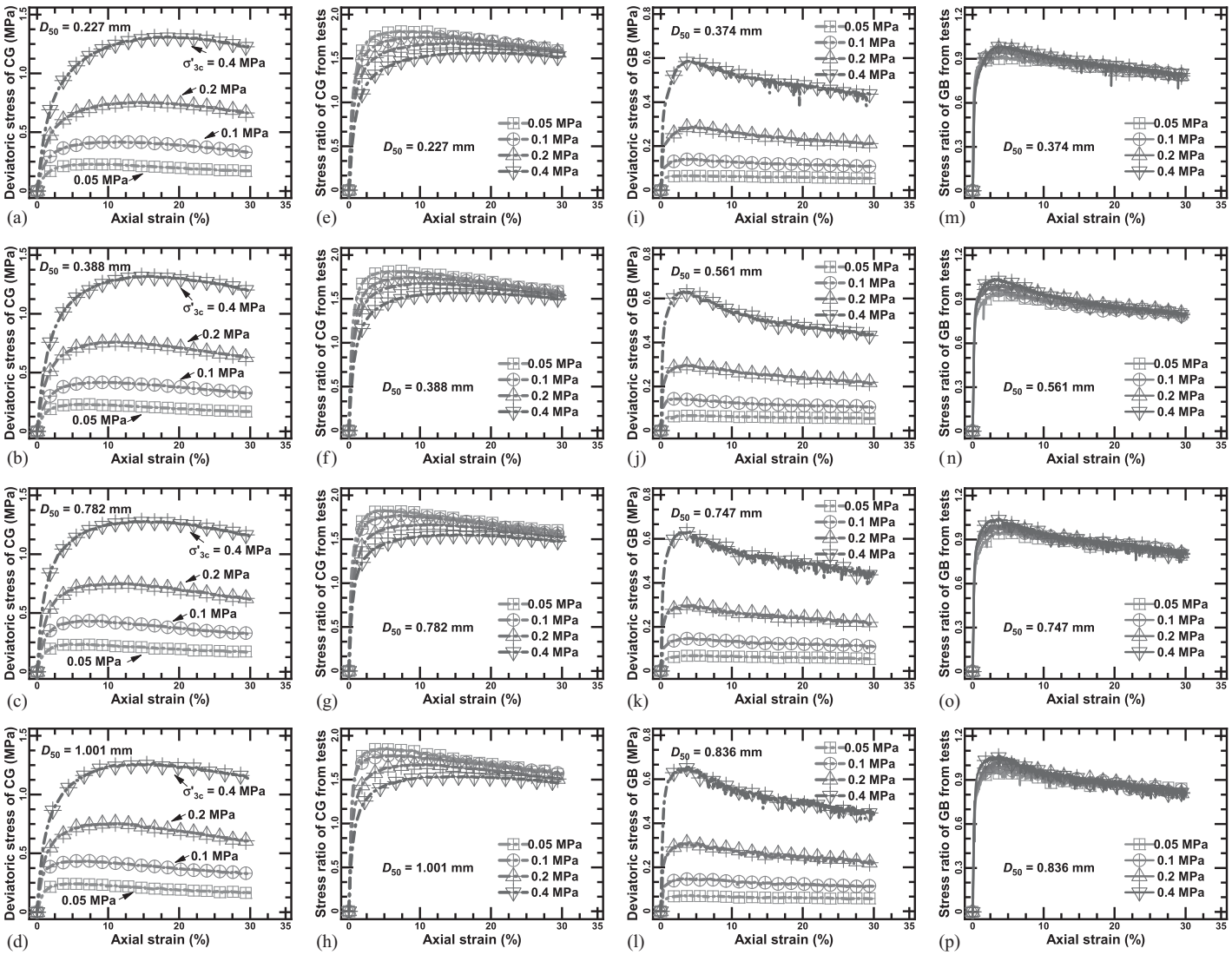

Fig. 2. Evolution of the stress–strain relationship from monotonic drained triaxial shear tests for different values of σ'_{3c}: (a–h) responses of the angular CG sands for a given D_{50}; and (i–p) responses of the rounded GB sands for a given D_{50}.

subrounded GB sands exhibiting larger q_{max}, q_{rs}, and ε_{rs}^{v} than the rounded GB sands, may be attributed to the small difference in particle shape.

Stress–Dilatancy Responses and Discussion

Based on previous studies (De Josselin De Jong 1976; Salgado et al. 2000), the maximum friction angle used in this study was defined as $\phi'_{max} = \arcsin[(n_{max}-1)/(n_{max}+1)]$, where n_{max} = maximum ratio of the major principal effective stress to the minor principal effective stress; and the maximum dilation angle is defined as $\psi_{max} = \arcsin[-m_{max}/(2-m_{max})]$, where m_{max} = maximum ratio of the volumetric strain increment to the axial strain increment. All test data on strength and dilatancy for the angular CG and rounded GB sands in the present study are shown in Figs. 6(a–i). Fig. 6(a) presents the variations in ϕ'_{max} with D_{50} and σ'_{3c} for the angular CG sands, which indicates that a decrease in σ'_{3c} led to a significant increase in the ϕ'_{max} of the angular CG sands, from approximately 38° at $\sigma'_{3c} = 0.4$ MPa to over 44° at $\sigma'_{3c} = 0.05$ MPa. By contrast, an increase in σ'_{3c} led to a small, but somewhat notable, increase in the ϕ'_{max} of the rounded GB sands [Fig. 6(b)]. For the angular CG sands, the ϕ'_{max} increased slightly with increasing D_{50} at low values of σ'_{3c}, but decreased marginally at high values of σ'_{3c} [Fig. 6(a)]. For example, the ϕ'_{max} increased slightly, from 44.3° to 45.2°, with D_{50} increasing from 0.227 to 1.001 mm at $\sigma'_{3c} = 0.05$ MPa, whereas the ϕ'_{max} decreased slightly, from 38.5° to 37.8°, as the D_{50} increased from 0.227 to 1.001 mm at $\sigma'_{3c} = 0.4$ MPa. The maximum difference in the ϕ'_{max} at a given σ'_{3c} was no more than 0.9° for the angular CG sands over the range in D_{50}. However, the rounded GB sands exhibited an increase in ϕ'_{max} with increasing D_{50} at all given confining pressures [Fig. 6(b)], with the maximum difference in ϕ'_{max} being 0.8° to 1.7° over the range of D_{50} values investigated. Figs. 6(c and d) present the experimentally derived surfaces for the ψ_{max} over the ranges in D_{50} and σ'_{3c} for the angular CG and rounded GB sands, respectively. For the angular CG sands in Fig. 6(c), the ψ_{max} increased with decreasing σ'_{3c}, indicating that the contribution of ψ_{max} to ϕ'_{max} increased with decreasing σ'_{3c}, which was verified from Fig. 6(a). By contrast, the ψ_{max} increased with increasing σ'_{3c} in the rounded GB sands [Fig. 6(d)], which explains, in part, the increased ϕ'_{max} with σ'_{3c} described in Fig. 6(b). In addition, increases in the D_{50} led to increases in the ψ_{max} for both of the sands, which is in line with previously reported test results (Bagherzadeh-

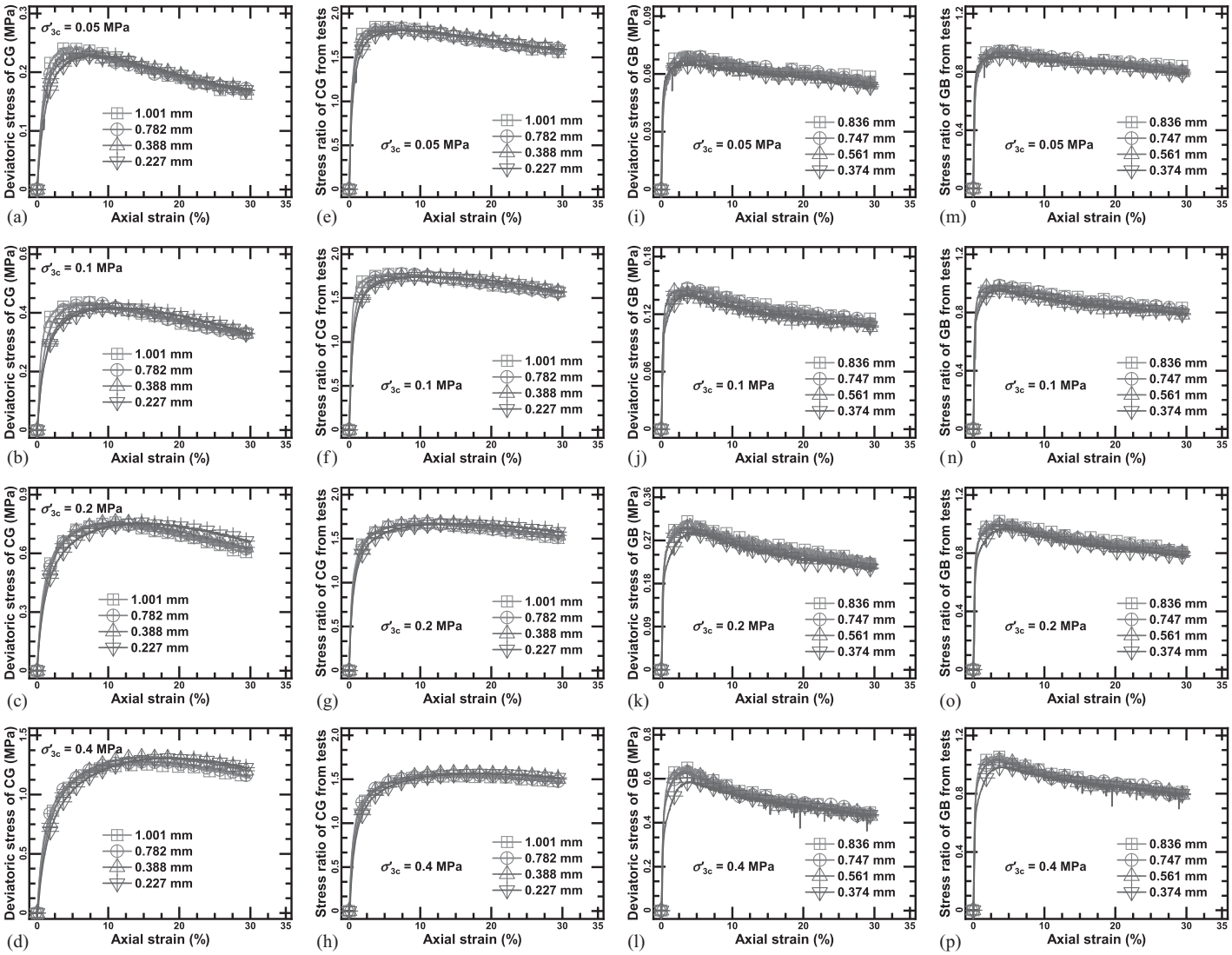

Fig. 3. Evolution of the stress–strain relationship from monotonic drained triaxial shear tests for different values of D_{50}: (a–h) responses of the angular CG sands for a given σ'_{3c}; and (i–p) responses of the rounded GB sands for a given σ'_{3c}.

Int. J. Geomech., 2023, 23(8): 04023117

Khalkhali and Mirghasemi 2009; Hamidi et al. 2012; Dai et al. 2016; Ari and Akbulut 2022). For instance, the ψ_{max} of the angular CG sands shown in Fig. 6(c) increased from 11.0° to 14.7° as the D_{50} increased from 0.227 to 1.001 mm at $\sigma'_{3c} = 0.05$ MPa. For the angular CG sands, the maximum difference in the ψ_{max} at a given σ'_{3c} decreased from 3.7° to 1.3° as σ'_{3c} increased from 0.05 to 0.4 MPa, while the maximum difference in the ψ_{max} for the rounded GB sands was 1.7° at $\sigma'_{3c} = 0.4$ MPa. Therefore, the surface describing the variation in ψ_{max} with σ'_{3c} and D_{50} for the rounded GB sands [Fig. 6(d)] is significantly less curved than that for the angular CG sands [Fig. 6(c)]. Despite the ε_a being up to 30%, the triaxial specimens may not have achieved the critical state owing to the slight nonzero rate of volumetric strain observed in many of the tests, especially in the angular CG sands shown in Fig. 4. Based on the studies by Vaid and Sasitharan (1992), Amirpour Harehdasht et al. (2017), Xiao et al. (2019a), and Arda and Cinicioglu (2021), the intercept of the empirical stress–dilatancy relationship for sands, proposed by Bolton (1986), can be interpreted as ϕ'_{cs}, which can be expressed as $\phi'_{max} = \phi'_{cs} + \chi_d \psi_{max}$ and $\phi'_{ex} = \phi'_{max} - \phi'_{cs}$, where χ_d = dilatancy coefficient; and ϕ'_{ex} = excess friction angle. Figs. 6(e and f) illustrate the responses between ϕ'_{max}, D_{50}, and ψ_{max} for the angular CG and rounded GB sands, respectively. The slope of the fitted stress–dilatancy equation was 0.67 for the angular CG and rounded GB sands for all values of D_{50}, which indicates that the dilatancy coefficient, χ_d, is largely independent of particle size and shape. Similar magnitudes of χ_d, ranging from 0.6 to 0.7, have also been reported in other studies (Guo and Su 2007; Dai et al. 2016; Giampa et al. 2017; Giampa and Bradshaw 2018; Amirpour Harehdasht et al. 2019; Arda and Cinicioglu 2021). The calculated critical-state friction angle (ϕ'_{cs-cal}) for the angular CG sands, computed using Bolton's stress–dilatancy equation, was equal to 36.8°, 36.3°, 35.7°, and 35.5° for $D_{50} = 0.227$, 0.388, 0.782, and 1.001 mm, respectively, indicating a slight decrease in ϕ'_{cs-cal} with increasing D_{50}, which is in line with the finding by Vangla and Latha (2015) for angular sands. By contrast, in the rounded GB sands [Fig. 6(f)], the ϕ'_{cs-cal} increased slightly (e.g., 20.2° to 20.8°) with increasing D_{50}, from 0.374 to 0.836 mm. This phenomenon was also discovered by Dai et al. (2016) in rounded glass beads. The maximum difference in ϕ'_{cs} was 1.3° for the angular CG sands with the D_{50} ranging from 0.227 to 1.001 mm, and 0.6° for the rounded GB sands with the D_{50} ranging from 0.374 to 0.836 mm, respectively. These differences are much smaller than those reported by Vangla and Latha (2015) and Dai et al. (2016). Therefore, the effect of particle size

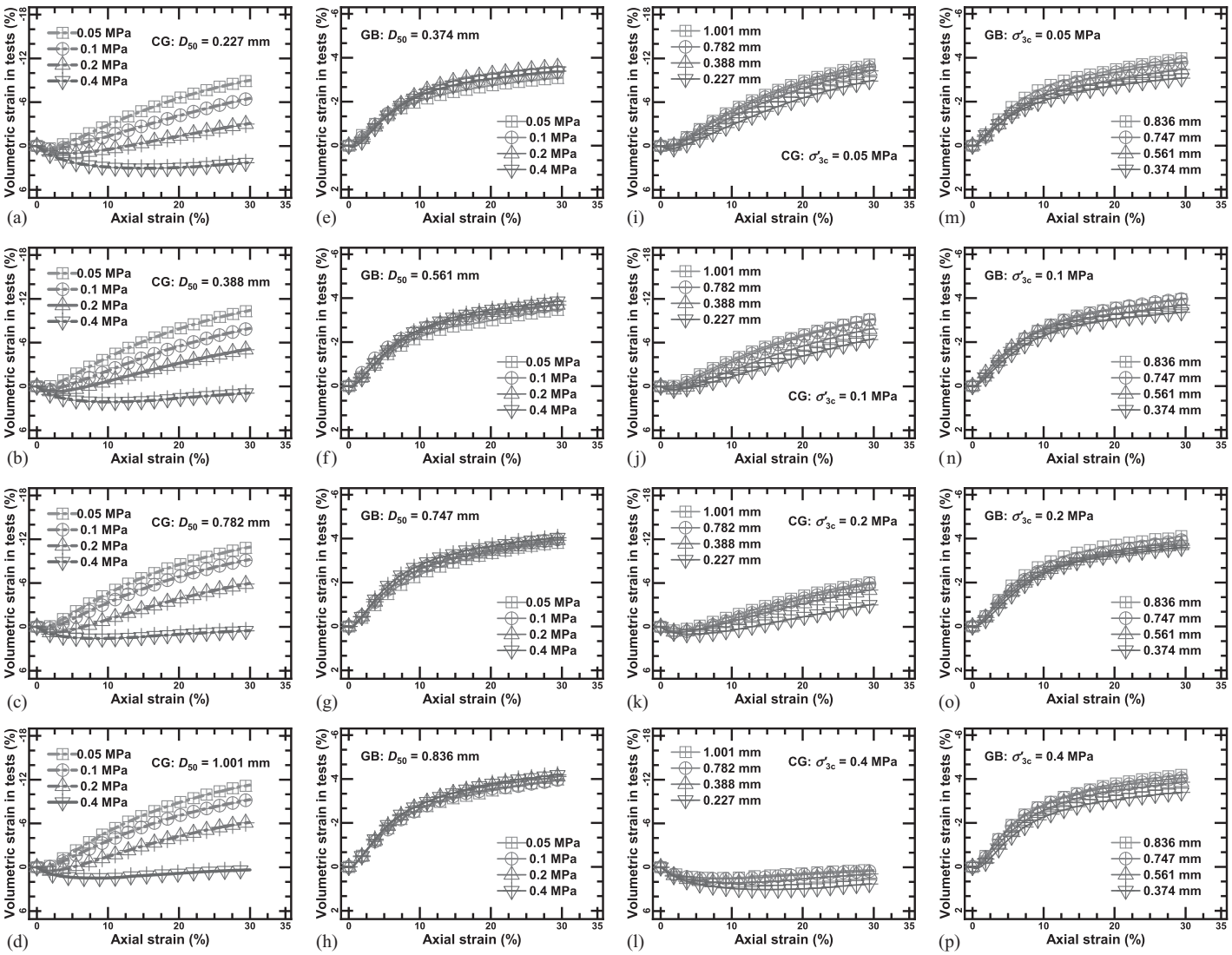

Fig. 4. Evolution of the volumetric deformation of the angular CG and rounded GB sands from monotonic drained triaxial shear tests: (a–h) responses for a given D_{50} for different values of σ'_{3c}; and (i–p) responses for different values of D_{50} for a given σ'_{3c}.

on ϕ'_{cs} can be neglected, similarly to the effect of gradation on ϕ'_{cs} (Yang and Luo 2018), although gradation can trigger liquefaction and the position of the critical-state line in the compression plane. Particle shape, however, is a significant factor affecting ϕ'_{cs}. The observed critical-state friction angle, ϕ'_{cs-obs}, inferred from the slope of the stress path in the $q-p'$ plane in the residual state corresponding to $\varepsilon_a \approx 30\%$, can be computed, assuming that the specimen nearly achieved the critical state. Also, based on the work by Schofield and Wroth (1968), its expression can be given as $\phi'_{cs-obs} = \arcsin[3\eta_{rs}/(6+\eta_{rs})]$, where η_{rs} = stress ratio at the residual state. This method facilitates a comparison of the two estimates of ϕ'_{ex} for each glass sand. The variations in ϕ'_{ex} with D_{50} and σ'_{3c} for the angular CG and rounded GB sands are presented in Figs. 6(g and h), respectively. As shown in Fig. 6(g), the ϕ'_{ex} calculated using ϕ'_{cs-cal} for the angular CG sands was larger than that computed using ϕ'_{cs-obs}, similar to the result obtained for the rounded GB sands shown in Fig. 6(h). Obviously, this observation can be explained by the triaxial specimens not having achieved the critical state. However, this comparison did validate the reliability of ϕ'_{cs} obtained from Bolton's stress–dilatancy equation. Fig. 6(i) presents the relationship between ϕ'_{ex} and $\psi_{\max}$ for all glass sands with different values of D_{50}, where all these data projected in the $\phi'_{ex}-\psi_{\max}$ plane can be linearly fitted by Bolton's stress–dilatancy equation. This phenomenon further indicates that the coefficient of Bolton's stress–dilatancy equation is constant for these glass sands over the range in D_{50} values investigated (with $R^2 = 0.998$).

Based on the particle-scale mechanism viewpoint (Oda 1972; Iwashita and Oda 2000), and components of the shear strength of sands (Guo and Su 2007), interparticle locking restrains relative sliding and rotation between particles in sands, which could help in forming a series of parallel particle columns, and thereby the main stress chains to support external loads. The particle columns became shorter as ε_a increased, such that some particles needed to be released from the particle columns during shear. It was noted that the interparticle locking capability was much higher in the angular CG sands than in the rounded GB sands. Therefore, the rounded particles slipped and were released from the particle columns more readily than the angular particles during shear, and the parallel particle columns composed of angular particles were more stable than those formed by rounded particles, implying that the shear strength of the angular CG sands was higher than that of the rounded GB sands, as indicated in Figs. 6(a and b). The effective diameter of the particle columns formed by the angular particles may have been larger than those formed by the rounded

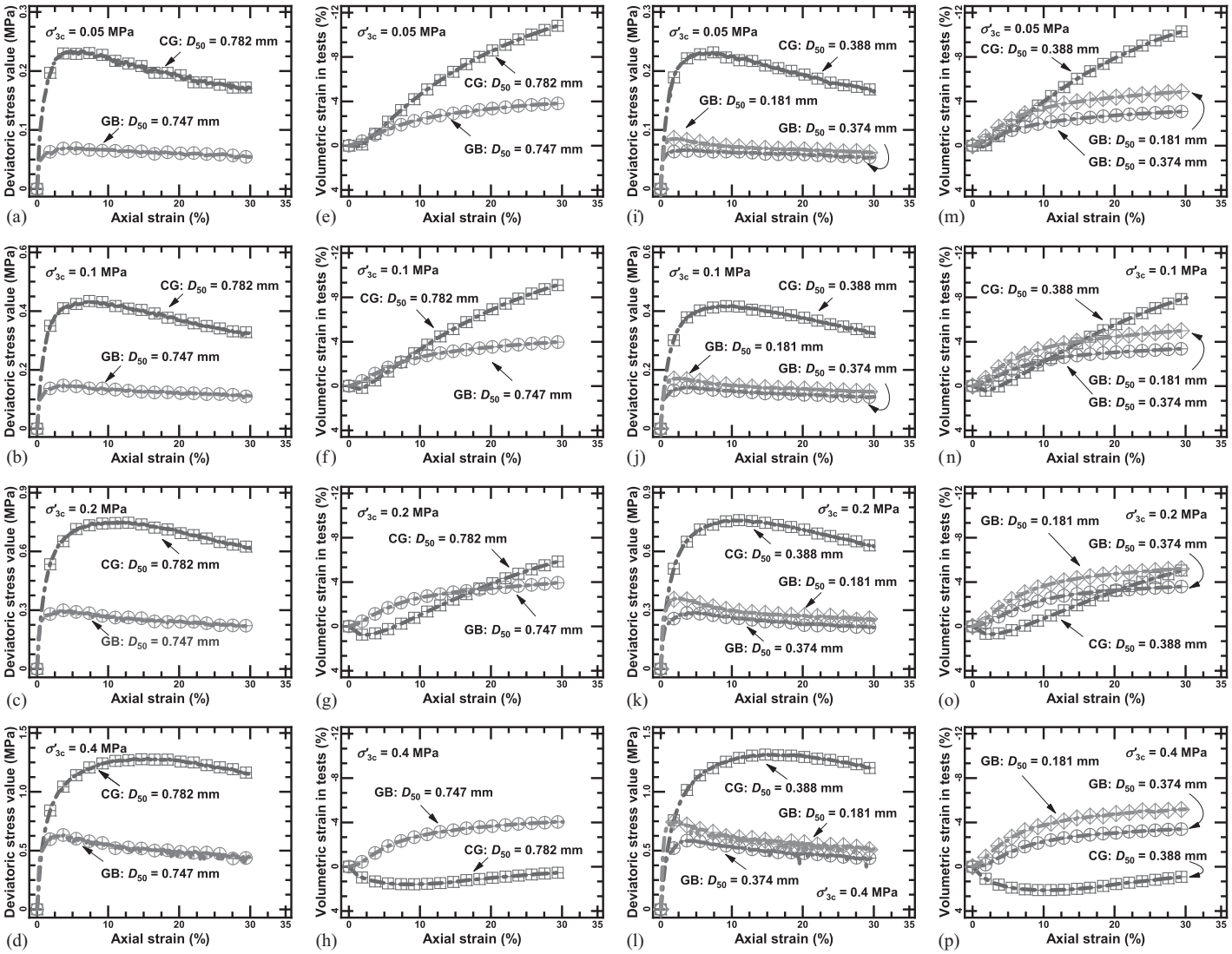

Fig. 5. Comparisons of the stress–strain relationships for the angular CG and subrounded/rounded GB sands from monotonic drained triaxial shear tests: (a–h) responses for $D_{50} = 0.747$–0.782 mm; and (i–p) responses for $D_{50} = 0.181$–0.388 mm.

particles, and the stability of the particle columns were higher for the angular CG sands than for the rounded GB sands. This suggests that the dilation of the angular CG sands during shearing should be higher than that of the rounded GB sands. However, as the confining pressure increased, the diameter and instability of the particle columns were more effectively suppressed for the angular CG sands than for the rounded GB sands. Consequently, the ψ_{max} of the angular CG sands at $\sigma'_{3c} = 0.4$ MPa was smaller than that of the rounded GB sands. Furthermore, the diameter of the effective particle columns could have increased, whereas the number of the effective particle columns could have decreased, as particle size increased, with the combined effect leading to a marginal to somewhat considerable increase in ϕ'_{max} and ψ_{max} at different levels of σ'_{3c} as the particle size increased, as shown in Figs. 6(a–d). Notably, increasing σ'_{3c} could effectively overwhelm the formation and deformation of particle columns composed of angular particles, with a different trend for ϕ'_{max} versus D_{50} in the angular CG sands being observed for $\sigma'_{3c} = 0.4$ MPa, as shown in Fig. 6(a). However, the maximum difference in ϕ'_{max} was as low as 0.7° for the angular CG sands at $\sigma'_{3c} = 0.4$ MPa. Therefore, in this study, we have demonstrated that, while particle size can contribute to differences in the shear strength and dilatancy responses of sands, the effect is marginal. Nevertheless, it is particle shape that strongly contributes to differences in the shear strength and dilation responses of sands. The angular CG sands possessed higher ϕ'_{max} and ψ_{max} than the rounded GB sands (except for at $\sigma'_{3c} = 0.4$ MPa), as well as ϕ'_{cs}. For example, for $D_{50} = 0.782$ mm, the ϕ'_{cs-cal} (=35.7°) of the angular CG sands was 1.7 times larger than that of the rounded GB sands for similar D_{50} ($\phi'_{cs-cal} = 20.7°$, $D_{50} = 0.747$ mm), whereas the difference in O_R was large ($O_R = 0.779$ and 0.935 for the angular CG and rounded GB sands, respectively). In another example, using a smaller D_{50}, the ϕ'_{cs-cal} for the angular CG sands was 1.8 times larger than that of the rounded GB sands for $D_{50} = 0.388$ and 0.374 mm, respectively. However, the corresponding O_R was significantly different, with $O_R = 0.781$ and 0.929 for the angular CG and rounded GB sands, respectively. These findings are generally consistent with the results from previous studies (Suh et al. 2017; Sarkar et al. 2019; Lashkari et al. 2020; Arda and Cinicioglu 2021; Deng et al. 2021; Shi et al. 2021; Wang et al. 2021; Wu et al. 2021b; Nie et al. 2022). For instance, Yang and Luo (2018) suggested a linear reduction in ϕ'_{cs} with O_R for Fujian sand mixed with different percentages of the CG and GB sands. Alshibli and

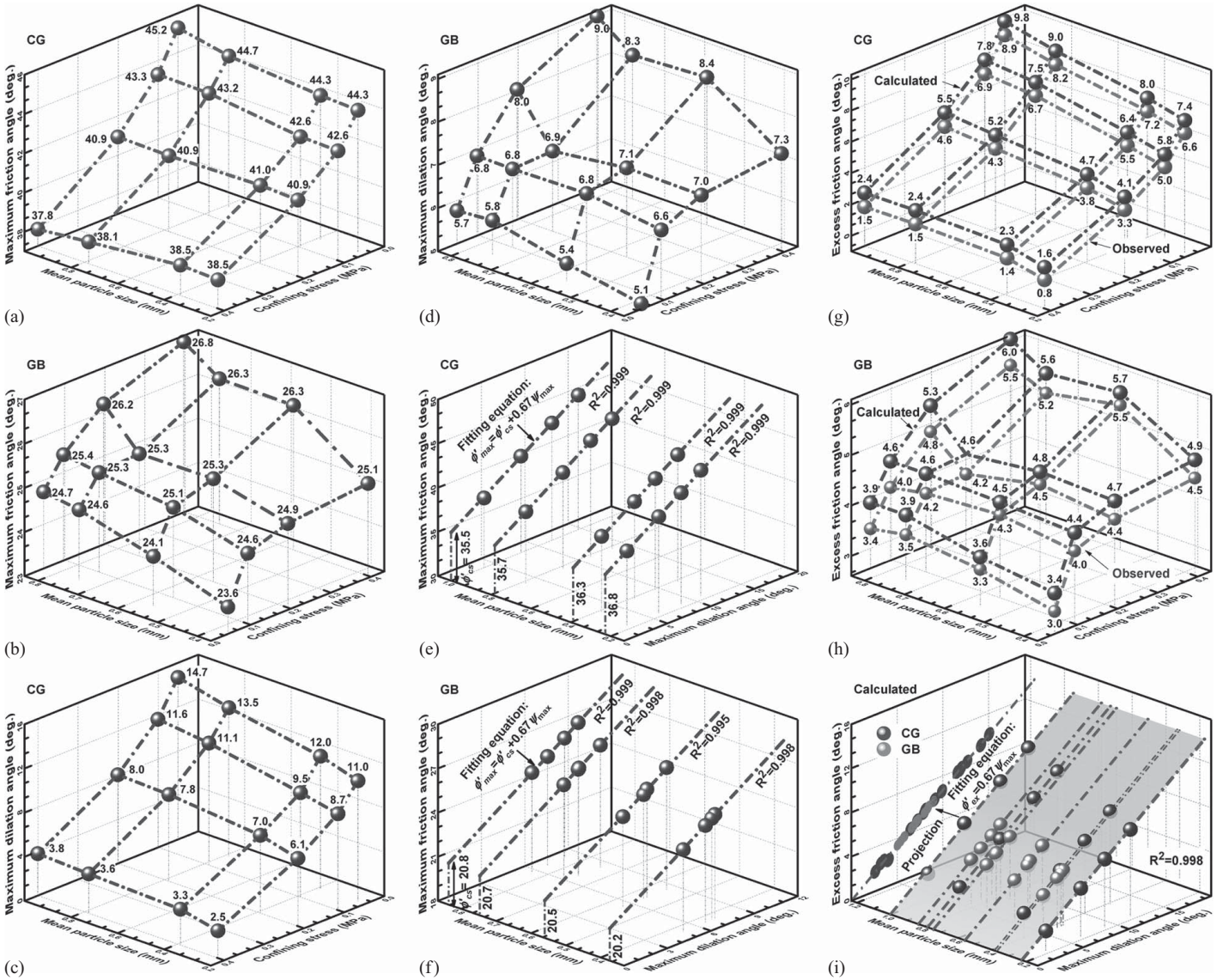

Fig. 6. Responses of the angular CG and rounded GB sands at the maximum stress state: (a–d) variations in observed friction and dilatancy angles; (e and f) stress–dilatancy relationship; and (g–i) comparisons between the calculated and observed friction angle.

Cil (2018) found that the ϕ'_{cs} of the GB sands was smaller than those of Ottawa sand and Columbia grout sand, for example, although the values of ϕ'_{cs} for the GB sands were notably larger than those of the GB sands in this study or in other studies (Cho et al. 2006; Altuhafi et al. 2016; Amirpour Harehdasht et al. 2017; Wu et al. 2017; Sarkar et al. 2019; Xiao et al. 2019a). Deng et al. (2021) also confirmed that the ϕ'_{cs} of Pasabahce silica sand decreases linearly with an increase in roundness. Therefore, our final conclusions regarding whether or not particle size affects the shear strength and dilatancy of sands are limited due to the range in particle sizes in the present study. A wider suite of laboratory tests on sands with a larger range of particle sizes for a given particle shape will be necessary to establish whether or not the strength of sands is influenced by particle size.

Conclusions and Remarks

A series of deliberately designed triaxial tests were conducted on CG and GB sands to introduce the effects of particle size and particle shape on the strength and dilatancy of the sands. The maximum and minimum void ratios (e_{max} and e_{min}) were significantly affected by particle shape. The angular CG sands exhibited a much larger e_{max} and e_{min} than the subrounded/rounded GB sands. With increasing mean particle size, D_{50}, both the e_{max} and e_{min} of the angular CG sands decreased while those of the rounded GB sands showed no evident changes. All CG and GB sands at an initial relative density of 60% showed typical strain-softening and dilative behaviors for confining pressures (σ'_{3c}) from 0.05 to 0.4 MPa. In addition, the angular CG sands exhibited a dramatic variation in both their stress–strain relationship and volumetric response with different confining pressures, whereas the rounded GB sands showed a more obvious stick–slip behavior and a nearly constant dilative behavior with increasing confining pressure. Under other similar test conditions, an increase in D_{50} led to an evident increase in the maximum dilatancy angle (ψ_{max}) and volume expansion in the residual state ($|\varepsilon^v_{rs}|$) in the angular CG sands, but only a slight increase in the ψ_{max} and $|\varepsilon^v_{rs}|$ in the rounded GB sands. However, as the D_{50} increased, the maximum friction angle (ϕ'_{max}) of the angular CG sands increased at $\sigma'_{3c} \leq 0.1$ MPa, but decreased at $\sigma'_{3c} \geq 0.2$ MPa, and the critical-state friction angle (ϕ'_{cs}) of the angular CG sands was found to decrease, whereas both the ϕ'_{max} and ϕ'_{cs} of the rounded GB sands exhibited a marginal increase. In addition, the effect of particle shape on the stress–dilatancy responses of medium-dense glass sands was further established. At a given σ'_{3c} and similar D_{50}, the order of values of ϕ'_{max} and ϕ'_{cs} was rounded GB sands < subrounded GB sands < angular CG sands, corresponding to a decreasing overall regularity, O_R. Bolton's stress–dilatancy equation was examined for the angular CG and rounded GB sands, where the slope (i.e., the dilatancy coefficient) was constant for different values of D_{50} and O_R, but the intercept (i.e., the calculated critical-state friction angle) varied slightly with D_{50}.

Data Availability Statement

All data, models, and code generated or used during the study appear in the published article. The optical images for displacement data used for validation, and the recorded videos of specimens of crushed glass and glass beads taken during the drained triaxial shear tests, the SEM images of particles of crushed glass and glass beads, the additional repeated data used for validation, possible discussions and comparisons, and other equations and procedures used for interpretations are available from the corresponding author upon reasonable request.

Acknowledgments

The authors would like to acknowledge the financial support of the National Nature Science Foundation of China (Grant Nos. 51922024 and 52078085). T.M.E. was supported by the National Science Foundation (NSF) (Grant No. CMMI-1933355) during the course of this work; that support is gratefully acknowledged. We would like to thank Mr. Y. Sun, Mr. Y. Zhang, Mr. H. M. Lu, Mr. W. Zhou, and Mr. Y. Y. Ling for their assistance in the preparation of the glass-sand specimens and the mechanical experiments, and Dr. H. R. Wu, Dr. J. Q. Shi, Dr. X. Jiang, and Dr. Z. C. Sun for their valuable suggestions on the analysis of the responses and mechanisms concerning the shear strength and dilation of the glass-sand specimens. We also appreciated the useful discussions with the former students on this team, including Miss L. H. Long, Mr. H. Zhou, Mr. H. Chen, Mr. B. W. Nan, Mr. Z. X. Yuan, and Mr. P. Chen. Finally, special thanks go to the Key Laboratory of New Technology for Construction of Cities in Mountain Area, and the Analytical and Testing Center of Chongqing University for use of their instruments for this study.

References

Adjemian, F., and P. Evesque. 2004. "Experimental study of stick-slip behaviour." *Int. J. Numer. Anal. Methods Geomech.* 28 (6): 501–530. https://doi.org/10.1002/nag.350.

Al-Hussaini, M. 1983. "Effect of particle size and strain conditions on the strength of crushed basalt." *Can. Geotech. J.* 20 (4): 706–717. https://doi.org/10.1139/t83-077.

Alikarami, R., E. Ando, M. Gkiousas-Kapnisis, A. Torabi, and G. Viggiani. 2015. "Strain localisation and grain breakage in sand under shearing at high mean stress: Insights from in situ X-ray tomography." *Acta Geotech.* 10 (1): 15–30. https://doi.org/10.1007/s11440-014-0364-6.

Alshibli, K. A., S. N. Batiste, and S. Sture. 2003. "Strain localization in sand: Plane strain versus triaxial compression." *J. Geotech. Geoenviron. Eng.* 129 (6): 483–494. https://doi.org/10.1061/(ASCE)1090-0241(2003)129:6(483).

Alshibli, K. A., and M. B. Cil. 2018. "Influence of particle morphology on the friction and dilatancy of sand." *J. Geotech. Geoenviron. Eng.* 144 (3): 04017118. https://doi.org/10.1061/(ASCE)GT.1943-5606.0001841.

Alshibli, K. A., M. F. Jarrar, A. M. Druckrey, and R. I. Al-Raoush. 2017. "Influence of particle morphology on 3D kinematic behavior and strain localization of sheared sand." *J. Geotech. Geoenviron. Eng.* 143 (2): 04016097. https://doi.org/10.1061/(ASCE)GT.1943-5606.0001601.

Alshibli, K. A., and L. E. Roussel. 2006. "Experimental investigation of slip-stick behaviour in granular materials." *Int. J. Numer. Anal. Methods Geomech.* 30 (14): 1391–1407. https://doi.org/10.1002/nag.517.

Altuhafi, F. N., M. R. Coop, and V. N. Georgiannou. 2016. "Effect of particle shape on the mechanical behavior of natural sands." *J. Geotech. Geoenviron. Eng.* 142 (12): 04016071. https://doi.org/10.1061/(ASCE)GT.1943-5606.0001569.

Altuhafi, F., C. O'Sullivan, and I. Cavarretta. 2013. "Analysis of an image-based method to quantify the size and shape of sand particles." *J. Geotech. Geoenviron. Eng.* 139 (8): 1290–1307. https://doi.org/10.1061/(ASCE)GT.1943-5606.0000855.

Amirpour Harehdasht, S., M. N. Hussien, M. Karray, V. Roubtsova, and M. Chekired. 2019. "Influence of particle size and gradation on shear strength–dilation relation of granular materials." *Can. Geotech. J.* 56 (2): 208–227. https://doi.org/10.1139/cgj-2017-0468.

Amirpour Harehdasht, S., M. Karray, M. N. Hussien, and M. Chekired. 2017. "Influence of particle size and gradation on the stress-dilatancy behavior of granular materials during drained triaxial compression."

Int. J. Geomech. 17 (9): 04017077. https://doi.org/10.1061/(ASCE)GM.1943-5622.0000951.
Arda, C., and O. Cinicioglu. 2021. "Influence of grain shape on stress-dilatancy parameters." *Granular Matter* 23 (2): 22. https://doi.org/10.1007/s10035-021-01098-2.
Ari, A., and S. Akbulut. 2022. "Effect of particle size and shape on shear strength of sand-rubber granule mixtures." *Granular Matter* 24 (4): 126. https://doi.org/10.1007/s10035-022-01287-7.
ASTM. 2016a. *Standard test methods for minimum index density and unit weight of soils and calculation of relative density*. ASTM D4254-16. West Conshohocken, PA: ASTM.
ASTM. 2016b. *Test method for maximum index density and unit weight of soils using vibratory table*. ASTM D4253-16. West Conshohocken, PA: ASTM.
Bagherzadeh-Khalkhali, A., and A. A. Mirghasemi. 2009. "Numerical and experimental direct shear tests for coarse-grained soils." *Particuology* 7 (1): 83–91. https://doi.org/http://dx.doi.org/10.1016/j.partic.2008.11.006.
Bandini, V., and M. R. Coop. 2011. "The influence of particle breakage on the location of the critical state line of sands." *Soils Found.* 51 (4): 591–600. https://doi.org/10.3208/sandf.51.591.
Been, K., and M. G. Jefferies. 1985. "A state parameter for sands." *Géotechnique* 35 (2): 99–112. https://doi.org/10.1680/geot.1985.35.2.99.
Bolton, M. D. 1986. "The strength and dilatancy of sands." *Géotechnique* 36 (1): 65–78. https://doi.org/10.1680/geot.1986.36.1.65.
Carraro, J. A. H., M. Prezzi, and R. Salgado. 2009. "Shear strength and stiffness of sands containing plastic or nonplastic fines." *J. Geotech. Geoenviron. Eng.* 135 (9): 1167–1178. https://doi.org/10.1061/(ASCE)1090-0241(2009)135:9(1167).
Cavarretta, I., M. Coop, and C. O'Sullivan. 2010. "The influence of particle characteristics on the behaviour of coarse grained soils." *Géotechnique* 60 (6): 413–423. https://doi.org/10.1680/geot.2010.60.6.413.
Chakraborty, T., and R. Salgado. 2010. "Dilatancy and shear strength of sand at low confining pressures." *J. Geotech. Geoenviron. Eng.* 136 (3): 527–532. https://doi.org/10.1061/(ASCE)GT.1943-5606.0000237.
Charles, J. A., and K. S. Watts. 1980. "The influence of confining pressure on the shear strength of compacted rockfill." *Géotechnique* 30 (4): 353–367. https://doi.org/10.1680/geot.1980.30.4.353.
Chen, X., and J. Zhang. 2016a. "Effect of clay invasion on shear behavior and dilatancy of unbound aggregate subbase." *Transp. Geotech.* 6: 16–25. https://doi.org/http://dx.doi.org/10.1016/j.trgeo.2015.12.001.
Chen, X., and J. Zhang. 2016b. "Influence of relative density on dilatancy of clayey sand-fouled aggregates in large-scale triaxial tests." *J. Geotech. Geoenviron. Eng.* 142 (10): 06016011. https://doi.org/10.1061/(ASCE)GT.1943-5606.0001542.
Chen, Y., G. Ma, W. Zhou, D. Wei, Q. Zhao, Y. Zou, and G. Grasselli. 2021. "An enhanced tool for probing the microscopic behavior of granular materials based on X-ray micro-CT and FDEM." *Comput. Geotech.* 132: 103974. https://doi.org/10.1016/j.compgeo.2020.103974.
Cho, G.-C., J. Dodds, and J. C. Santamarina. 2006. "Particle shape effects on packing density, stiffness, and strength: Natural and crushed sands." *J. Geotech. Geoenviron. Eng.* 132 (5): 591–602. https://doi.org/10.1061/(ASCE)1090-0241(2006)132:5(591).
Chu, J. 1995. "An experimental examination of the critical state and other similar concepts for granular soils." *Can. Geotech. J.* 32 (6): 1065–1075. https://doi.org/10.1139/t95-104.
Chu, J., and W. K. Leong. 2001. "Pre-failure strain softening and pre-failure instability of sand: A comparative study." *Géotechnique* 51 (4): 311–321. https://doi.org/10.1680/geot.2001.51.4.311.
Chu, J., W. K. Leong, W. L. Loke, and D. Wanatowski. 2012. "Instability of loose sand under drained conditions." *J. Geotech. Geoenviron. Eng.* 138 (2): 207–216. https://doi.org/10.1061/(ASCE)GT.1943-5606.0000574.
Chu, J., and S.-C. R. Lo. 1994. "Asymptotic behaviour of a granular soil in strain path testing." *Géotechnique* 44 (1): 65–82. https://doi.org/10.1680/geot.1994.44.1.65.
Chu, J., S.-C. R. Lo, and I. K. Lee. 1992. "Strain-softening behavior of granular soil in strain-path testing." *J. Geotech. Eng.* 118 (2): 191–208. https://doi.org/10.1061/(ASCE)0733-9410(1992)118:2(191).
Chu, J., S.-C. R. Lo, and I. K. Lee. 1993. "Instability of granular soils under strain path testing." *J. Geotech. Eng.* 119 (5): 874–892. https://doi.org/10.1061/(ASCE)0733-9410(1993)119:5(874).
Chu, J., and D. Wanatowski. 2008. "Instability conditions of loose sand in plane strain." *J. Geotech. Geoenviron. Eng.* 134 (1): 136–142. https://doi.org/10.1061/(ASCE)1090-0241(2008)134:1(136).
Chu, J., and D. Wanatowski. 2009. "Effect of loading mode on strain softening and instability behavior of sand in plane-strain tests." *J. Geotech. Geoenviron. Eng.* 135 (1): 108–120. https://doi.org/10.1061/(ASCE)1090-0241(2009)135:1(108).
Ciantia, M. O., and C. O'Sullivan. 2020. "Calculating the state parameter in crushable sands." *Int. J. Geomech.* 20 (7): 04020095. https://doi.org/10.1061/(ASCE)GM.1943-5622.0001707.
Cinicioglu, O., and A. Abadkon. 2015. "Dilatancy and friction angles based on in situ soil conditions." *J. Geotech. Geoenviron. Eng.* 141 (4): 06014019. https://doi.org/10.1061/(ASCE)GT.1943-5606.0001272.
Cubrinovski, M., and K. Ishihara. 2002. "Maximum and minimum void ratio characteristics of sands." *Soils Found.* 42 (6): 65–78. https://doi.org/10.3208/sandf.42.6_65.
Cui, D., W. Wu, W. Xiang, T. Doanh, Q. Chen, S. Wang, Q. Liu, and J. Wang. 2017. "Stick-slip behaviours of dry glass beads in triaxial compression." *Granular Matter* 19 (1): 1. https://doi.org/10.1007/s10035-016-0682-5.
Dai, B. B., J. Yang, and C. Y. Zhou. 2016. "Observed effects of interparticle friction and particle size on shear behavior of granular materials." *Int. J. Geomech.* 16 (1): 04015011. https://doi.org/10.1061/(ASCE)GM.1943-5622.0000520.
Daouadji, A., and P.-Y. Hicher. 2010. "An enhanced constitutive model for crushable granular materials." *Int. J. Numer. Anal. Methods Geomech.* 34 (6): 555–580. https://doi.org/10.1002/nag.815.
De Josselin De Jong, G. 1976. "Rowe's stress—dilatancy relation based on friction." *Géotechnique* 26 (3): 527–534. https://doi.org/10.1680/geot.1976.26.3.527.
Deng, Y., Y. Yilmaz, A. Gokce, and C. S. Chang. 2021. "Influence of particle size on the drained shear behavior of a dense fluvial sand." *Acta Geotech.* 16 (7): 2071–2088. https://doi.org/10.1007/s11440-021-01143-7.
Esposito, M. P. III, and R. D. Andrus. 2017. "Peak shear strength and dilatancy of a Pleistocene age sand." *J. Geotech. Geoenviron. Eng.* 143 (1): 04016079. https://doi.org/10.1061/(ASCE)GT.1943-5606.0001582.
Frossard, E., W. Hu, C. Dano, and P.-Y. Hicher. 2012. "Rockfill shear strength evaluation: A rational method based on size effects." *Géotechnique* 62 (5): 415–427. https://doi.org/10.1680/geot.10.P.079.
Fukushima, S., and F. Tatsuoka. 1984. "Strength and deformation characteristics of saturated sand at extremely low pressures." *Soils Found.* 24 (4): 30–48. https://doi.org/10.3208/sandf1972.24.4_30.
Giampa, J. R., and A. S. Bradshaw. 2018. "A simple method for assessing the peak friction angle of sand at very low confining pressures." *Geotech. Test. J.* 41 (4): 20170134. https://doi.org/10.1520/GTJ20170134.
Giampa, J. R., A. S. Bradshaw, and J. A. Schneider. 2017. "Influence of dilation angle on drained shallow circular anchor uplift capacity." *Int. J. Geomech.* 17 (2): 04016056. https://doi.org/10.1061/(ASCE)GM.1943-5622.0000725.
Gong, J., and J. Liu. 2017. "Effect of aspect ratio on triaxial compression of multi-sphere ellipsoid assemblies simulated using a discrete element method." *Particuology* 32: 49–62. https://doi.org/10.1016/j.partic.2016.07.007.
Gong, J., Z. Nie, Y. Zhu, Z. Liang, and X. Wang. 2019. "Exploring the effects of particle shape and content of fines on the shear behavior of sand-fines mixtures via the DEM." *Comput. Geotech.* 106: 161–176. https://doi.org/10.1016/j.compgeo.2018.10.021.
Graton, L. C., and H. J. Fraser. 1935. "Systematic packing of spheres: With particular relation to porosity and permeability." *J. Geol.* 43 (8): 785–909. https://doi.org/10.1086/624386.
Guida, G., D. Sebastiani, F. Casini, and S. Miliziano. 2019. "Grain morphology and strength dilatancy of sands." *Géotechnique Lett.* 9 (4): 245–253. https://doi.org/10.1680/jgele.18.00199.

Guo, P., and X. Su. 2007. "Shear strength, interparticle locking, and dilatancy of granular materials." *Can. Geotech. J.* 44 (5): 579–591. https://doi.org/10.1139/T07-010.

Hamidi, A., E. Azini, and B. Masoudi. 2012. "Impact of gradation on the shear strength-dilation behavior of well graded sand-gravel mixtures." *Sci. Iran.* 19 (3): 393–402. https://doi.org/10.1016/j.scient.2012.04.002.

Hanna, A. 2001. "Determination of plane-strain shear strength of sand from the results of triaxial tests." *Can. Geotech. J.* 38 (6): 1231–1240. https://doi.org/10.1139/t01-064.

Hassan, N. A., N. S. Nguyen, D. Marot, and F. Bendahmane. 2022. "Consequences of scalping and scalping/replacement procedures on strength properties of coarse-grained gap-graded soils." *Can. Geotech. J.* 59 (10): 1819–1832. https://doi.org/10.1139/cgj-2021-0504.

Honkanadavar, N. P., and K. G. Sharma. 2014. "Testing and modeling the behavior of riverbed and blasted quarried rockfill materials." *Int. J. Geomech.* 14 (6): 04014028. https://doi.org/10.1061/(ASCE)GM.1943-5622.0000378.

Honkanadavar, N. P., and K. G. Sharma. 2016. "Modeling the triaxial behavior of riverbed and blasted quarried rockfill materials using hardening soil model." *J. Rock Mech. Geotech. Eng.* 8 (3): 350–365. https://doi.org/10.1016/j.jrmge.2015.09.007.

Indraratna, B., D. Ionescu, and H. D. Christie. 1998. "Shear behavior of railway ballast based on large-scale triaxial tests." *J. Geotech. Geoenviron. Eng.* 124 (5): 439–449. https://doi.org/10.1061/(ASCE)1090-0241(1998)124:5(439).

Iwashita, K., and M. Oda. 2000. "Micro-deformation mechanism of shear banding process based on modified distinct element method." *Powder Technol.* 109 (1): 192–205. https://doi.org/10.1016/S0032-5910(99)00236-3.

Jiang, M. D., Z. X. Yang, D. Barreto, and Y. H. Xie. 2018. "The influence of particle-size distribution on critical state behavior of spherical and non-spherical particle assemblies." *Granular Matter* 20 (4): 80. https://doi.org/10.1007/s10035-018-0850-x.

Kandasami, R. K., and T. G. Murthy. 2017. "Manifestation of particle morphology on the mechanical behaviour of granular ensembles." *Granular Matter* 19 (2): 21. https://doi.org/10.1007/s10035-017-0703-z.

Karatza, Z., E. Ando, S.-A. Papanicolopulos, J. Y. Ooi, and G. Viggiani. 2018. "Evolution of deformation and breakage in sand studied using X-ray tomography." *Géotechnique* 68 (2): 107–117. https://doi.org/10.1680/jgeot.16.P.208.

Keramatikerman, M., and A. Chegenizadeh. 2017. "Effect of particle shape on monotonic liquefaction: Natural and crushed sand." *Exp. Mech.* 57 (8): 1341–1348. https://doi.org/http://dx.doi.org/10.1007/s11340-017-0313-z.

Kolymbas, D., and W. Wu. 1990. "Recent results of triaxial tests with granular materials." *Powder Technol.* 60 (2): 99–119. https://doi.org/10.1016/0032-5910(90)80136-M.

Koval, G., F. Chevoir, J.-N. Roux, J. Sulem, and A. Corfdir. 2011. "Interface roughness effect on slow cyclic annular shear of granular materials." *Granular Matter* 13 (5): 525–540. https://doi.org/10.1007/s10035-011-0267-2.

Ladd, R. S. 1978. "Preparing test specimens using undercompaction." *Geotech. Test. J.* 1 (1): 16–23. https://doi.org/10.1520/GTJ10364J.

Lade, P. V., C. D. Liggio, and J. A. Yamamuro. 1998. "Effects of nonplastic fines on minimum and maximum void ratios of sand." *Geotech. Test. J.* 21 (4): 336–347. https://doi.org/10.1520/GTJ11373J.

Lam, W.-K., and F. Tatsuoka. 1988. "Effects of initial anisotropic fabric and σ2 on strength and deformation characteristics of sand." *Soils Found.* 28 (1): 89–106. https://doi.org/10.3208/sandf1972.28.89.

Lancelot, L., I. Shahrour, and M. Al Mahmoud. 2006. "Failure and dilatancy properties of sand at relatively low stresses." *J. Eng. Mech.* 132 (12): 1396–1399. https://doi.org/10.1061/(ASCE)0733-9399(2006)132:12(1396).

Lashkari, A., S. R. Falsafizadeh, P. T. Shourijeh, and M. J. Alipour. 2020. "Instability of loose sand in constant volume direct simple shear tests in relation to particle shape." *Acta Geotech.* 15 (9): 2507–2527. https://doi.org/10.1007/s11440-019-00909-4.

Li, X. S., and Y. F. Dafalias. 2000. "Dilatancy for cohesionless soils." *Géotechnique* 50 (4): 449–460. https://doi.org/10.1680/geot.2000.50.4.449.

Li, Y. 2013. "Effects of particle shape and size distribution on the shear strength behavior of composite soils." *Bull. Eng. Geol. Environ.* 72 (3): 371–381. https://doi.org/10.1007/s10064-013-0482-7.

Li, Y., R. Huang, L. S. Chan, and J. Chen. 2013. "Effects of particle shape on shear strength of clay-gravel mixture." *KSCE J. Civ. Eng.* 17 (4): 712–717. https://doi.org/10.1007/s12205-013-0003-z.

Liang, H., Y. Shen, J. Xu, and S. Chen. 2022. "Multiscale morphological effects on stress-dilation behaviors of natural sands: A 3D printing simulation method." *J. Eng. Mech.* 148 (9): 04022046. https://doi.org/10.1061/(ASCE)EM.1943-7889.0002128.

Liu, M., Y. Zhang, and H. Zhu. 2017. "3D elastoplastic model for crushable soils with explicit formulation of particle crushing." *J. Eng. Mech.* 143 (12): 04017140. https://doi.org/10.1061/(ASCE)EM.1943-7889.0001361.

Marschi, N. D., C. K. Chan, and H. B. Seed. 1972. "Evaluation of properties of rockfill materials." *J. Soil Mech. Found. Div.* 98 (1): 95–114. https://doi.org/10.1061/JSFEAQ.0001735.

Miura, K., K. Maeda, M. Furukawa, and S. Toki. 1998. "Mechanical characteristics of sands with different primary properties." *Soils Found.* 38 (4): 159–172. https://doi.org/10.3208/sandf.38.4_159.

Muir Wood, D., and K. Maeda. 2008. "Changing grading of soil: Effect on critical states." *Acta Geotech.* 3 (1): 3–14. https://doi.org/10.1007/s11440-007-0041-0.

Murthy, T. G., D. Loukidis, J. A. H. Carraro, M. Prezzi, and R. Salgado. 2007. "Undrained monotonic response of clean and silty sands." *Géotechnique* 57 (3): 273–288. https://doi.org/10.1680/geot.2007.57.3.273.

Ng, T.-T., W. Zhou, and X.-L. Chang. 2017. "Effect of particle shape and fine content on the behavior of binary mixture." *J. Eng. Mech.* 143 (1): C4016008. https://doi.org/10.1061/(ASCE)EM.1943-7889.0001070.

Nguyen, H. B. K., M. M. Rahman, and A. B. Fourie. 2020. "Effect of particle shape on constitutive relation: DEM study." *J. Geotech. Geoenviron. Eng.* 146 (7): 04020058. https://doi.org/10.1061/(ASCE)GT.1943-5606.0002278.

Ni, Q., T. S. Tan, G. R. Dasari, and D. W. Hightf. 2004. "Contribution of fines to the compressive strength of mixed soils." *Géotechnique* 54 (9): 561–569. https://doi.org/10.1680/geot.2004.54.9.561.

Nie, J.-Y., J. Zhao, Y.-F. Cui, and D.-Q. Li. 2022. "Correlation between grain shape and critical state characteristics of uniformly graded sands: A 3D DEM study." *Acta Geotech.* 17 (7): 2783–2798. https://doi.org/10.1007/s11440-021-01362-y.

Oda, M. 1972. "Initial fabrics and their relations to mechanical properties of granular material." *Soils Found.* 12 (1): 17–36. https://doi.org/10.3208/sandf1960.12.17.

Ovalle, C., and C. Dano. 2020. "Effects of particle size-strength and size-shape correlations on parallel grading scaling." *Géotechnique Lett.* 10 (2): 191–197. https://doi.org/10.1680/jgele.19.00095.

Ovalle, C., E. Frossard, C. Dano, W. Hu, S. Maiolino, and P.-Y. Hicher. 2014. "The effect of size on the strength of coarse rock aggregates and large rockfill samples through experimental data." *Acta Mech.* 225 (Aug): 2199–2216. https://doi.org/10.1007/s00707-014-1127-z.

Rahman, M. M., and S. R. Lo. 2014. "Undrained behavior of sand-fines mixtures and their state parameter." *J. Geotech. Geoenviron. Eng.* 140 (7): 04014036. https://doi.org/10.1061/(ASCE)GT.1943-5606.0001115.

Rahman, M. M., S. R. Lo, and M. A. L. Baki. 2011. "Equivalent granular state parameter and undrained behaviour of sand-fines mixtures." *Acta Geotech.* 6 (4): 183–194. https://doi.org/10.1007/s11440-011-0145-4.

Salgado, R., P. Bandini, and A. Karim. 2000. "Shear strength and stiffness of silty sand." *J. Geotech. Geoenviron. Eng.* 126 (5): 451–462. https://doi.org/10.1061/(ASCE)1090-0241(2000)126:5(451).

Sarkar, D., M. Goudarzy, and D. König. 2019. "An interpretation of the influence of particle shape on the mechanical behavior of granular material." *Granular Matter* 21 (3): 53. https://doi.org/10.1007/s10035-019-0909-3.

Schofield, A. N., and C. P. Wroth. 1968. *Critical state soil mechanics*. London: MacGraw-Hill.

Shi, J., Y. Xiao, J. Hu, H. Wu, H. Liu, and W. Haegeman. 2022. "Small-strain shear modulus of calcareous sand under anisotropic

consolidation." *Can. Geotech. J.* 59 (6): 878–888. https://doi.org/10.1139/cgj-2021-0329.
Shi, X. S., K. Liu, and J. Yin. 2021. "Effect of initial density, particle shape, and confining stress on the critical state behavior of weathered gap-graded granular soils." *J. Geotech. Geoenviron. Eng.* 147 (2): 04020160. https://doi.org/10.1061/(ASCE)GT.1943-5606.0002449.
Simoni, A., and G. T. Houlsby. 2006. "The direct shear strength and dilatancy of sand–gravel mixtures." *Geotech. Geol. Eng.* 24: 523–549. https://doi.org/10.1007/s10706-004-5832-6.
Sitharam, T. G., and M. S. Nimbkar. 2000. "Micromechanical modelling of granular materials: Effect of particle size and gradation." *Geotech. Geol. Eng.* 18 (2): 91–117. https://doi.org/10.1023/A:1008982027109.
Suh, H. S., K. Y. Kim, J. Lee, and T. S. Yun. 2017. "Quantification of bulk form and angularity of particle with correlation of shear strength and packing density in sands." *Eng. Geol.* 220: 256–265. https://doi.org/http://dx.doi.org/10.1016/j.enggeo.2017.02.015.
Tarantino, A., and A. F. L. Hyde. 2005. "An experimental investigation of work dissipation in crushable materials." *Géotechnique* 55 (8): 575–584. https://doi.org/10.1680/geot.2005.55.8.575.
Tatsuoka, F., M. Sakamoto, T. Kawamura, and S. Fukushima. 1986. "Strength and deformation characteristics of sand in plane strain compression at extremely low pressures." *Soils Found.* 26 (1): 65–84. https://doi.org/10.3208/sandf1972.26.65.
Thakur Mohmad, M., and D. Penumadu. 2021. "Influence of friction and particle morphology on triaxial shearing of granular materials." *J. Geotech. Geoenviron. Eng.* 147 (11): 04021118. https://doi.org/10.1061/(ASCE)GT.1943-5606.0002634.
Tovar-Valencia Ruben, D., A. Galvis-Castro, R. Salgado, and M. Prezzi. 2018. "Effect of surface roughness on the shaft resistance of displacement model piles in sand." *J. Geotech. Geoenviron. Eng.* 144 (3): 04017120. https://doi.org/10.1061/(ASCE)GT.1943-5606.0001828.
Vaid, Y. P., and S. Sasitharan. 1992. "The strength and dilatancy of sand." *Can. Geotech. J.* 29 (3): 522–526. https://doi.org/10.1139/t92-058.
Vangla, P., and G. M. Latha. 2015. "Influence of particle size on the friction and interfacial shear strength of sands of similar morphology." *Int. J. Geosynth. Ground Eng.* 1 (1): 6. https://doi.org/10.1007/s40891-014-0008-9.
Varadarajan, A., K. G. Sharma, S. M. Abbas, and A. K. Dhawan. 2006. "Constitutive model for rockfill materials and determination of material constants." *Int. J. Geomech.* 6 (4): 226–237. https://doi.org/10.1061/(ASCE)1532-3641(2006)6:4(226).
Varadarajan, A., K. G. Sharma, K. Venkatachalam, and A. K. Gupta. 2003. "Testing and modeling two rockfill materials." *J. Geotech. Geoenviron. Eng.* 129 (3): 206–218. https://doi.org/10.1061/(ASCE)1090-0241(2003)129:3(206).
Wan, R. G., and P. J. Guo. 1998. "A simple constitutive model for granular soils: Modified stress-dilatancy approach." *Comput. Geotech.* 22 (2): 109–133. https://doi.org/10.1016/S0266-352X(98)00004-4.
Wan, R. G., and P. J. Guo. 1999. "A pressure and density dependent dilatancy model for granular materials." *Soils Found.* 39 (6): 1–11. https://doi.org/10.3208/sandf.39.6_1.
Wanatowski, D., and J. Chu. 2007. "Static liquefaction of sand in plane strain." *Can. Geotech. J.* 44 (3): 299–313. https://doi.org/10.1139/t06-078.
Wang, R., G. Pinzón, E. Andò, and G. Viggiani. 2022. "Modeling combined fabric evolution in an anisometric granular material driven by particle-scale x-ray measurements." *J. Eng. Mech.* 148 (1): 04021120. https://doi.org/10.1061/(ASCE)EM.1943-7889.0002032.
Wang, X., Z. Nie, J. Gong, and Z. Liang. 2021. "Random generation of convex aggregates for DEM study of particle shape effect." *Constr. Build. Mater.* 268: 121468. https://doi.org/10.1016/j.conbuildmat.2020.121468.
Wei, H.-Z., W.-J. Xu, X.-F. Xu, Q.-S. Meng, and C.-F. Wei. 2018. "Mechanical properties of strongly weathered rock-soil mixtures with different rock block contents." *Int. J. Geomech.* 18 (5): 12. https://doi.org/10.1061/(ASCE)GM.1943-5622.0001131.
Wei, L. M., and J. Yang. 2014. "On the role of grain shape in static liquefaction of sand–fines mixtures." *Géotechnique* 64 (9): 740–745. https://doi.org/10.1680/geot.14.T.013.
Wu, H., W. Wu, W. Liang, F. Dai, H. Liu, and Y. Xiao. 2023. "3D DEM modeling of biocemented sand with fines as cementing agents." *Int. J. Numer. Anal. Methods Geomech.* 47: 212–240. https://doi.org/10.1002/nag.3466.
Wu, K., N. Abriak, F. Becquart, P. Pizette, S. Remond, and S. Liu. 2017. "Shear mechanical behavior of model materials samples by experimental triaxial tests: Case study of 4 mm diameter glass beads." *Granular Matter* 19 (4): 65. https://doi.org/10.1007/s10035-017-0753-2.
Wu, S., B. Li, and J. Chu. 2021a. "Stress-dilatancy behavior of MICP-treated sand." *Int. J. Geomech.* 21 (3): 04020264. https://doi.org/10.1061/(ASCE)gm.1943-5622.0001923.
Wu, Y., J. Cui, J. Huang, W. Zhang, N. Yoshimoto, and L. Wen. 2021b. "Correlation of critical state strength properties with particle shape and surface fractal dimension of clinker ash." *Int. J. Geomech.* 21 (6): 04021071. https://doi.org/10.1061/(ASCE)GM.1943-5622.0002027.
Xiao, Y., X. He, M. Zaman, G. Ma, and C. Zhao. 2022a. "Review of strength improvements of biocemented soils." *Int. J. Geomech.* 22 (11): 03122001. https://doi.org/10.1061/(ASCE)GM.1943-5622.0002565.
Xiao, Y., Y. Ling, J. Shi, Y. Sun, and H. Liu. 2022b. "Breakage and morphology of sands in drained shearing." *Int. J. Geomech.* 22 (9): 04022140. https://doi.org/10.1061/(ASCE)GM.1943-5622.000252.
Xiao, Y., and H. Liu. 2017. "Elastoplastic constitutive model for rockfill materials considering particle breakage." *Int. J. Geomech.* 17 (1): 04016041. https://doi.org/10.1061/(ASCE)GM.1943-5622.0000681.
Xiao, Y., L. Long, T. M. Evans, H. Zhou, H. Liu, and A. W. Stuedlein. 2019a. "Effect of particle shape on stress-dilatancy responses of medium-dense sands." *J. Geotech. Geoenviron. Eng.* 145 (2): 04018105. https://doi.org/10.1061/(ASCE)GT.1943-5606.0001994.
Xiao, Y., A. W. Stuedlein, J. Ran, T. M. Evans, L. Cheng, H. Liu, L. A. van Paassen, and J. Chu. 2019b. "Effect of particle shape on strength and stiffness of biocemented glass beads." *J. Geotech. Geoenviron. Eng.* 145 (11): 06019016. https://doi.org/10.1061/(ASCE)GT.1943-5606.0002165.
Xiao, Y., Y. Sun, H. Liu, J. Xiang, Q. Ma, and L. Long. 2017a. "Model predictions for behaviors of sand-nonplastic-fines mixtures using equivalent-skeleton void-ratio state index." *Sci. China Technol. Sci.* 60 (5): 878–892. https://doi.org/10.1007/s11431-016-9024-9.
Xiao, Y., Y. Sun, W. Zhou, J. Shi, and S. Desai Chandrakant. 2022c. "Evolution of particle shape produced by sand breakage." *Int. J. Geomech.* 22 (4): 04022003. https://doi.org/10.1061/(ASCE)GM.1943-5622.0002333.
Xiao, Y., C. Wang, Z. Zhang, H. Liu, and Z.-y. Yin. 2021a. "Constitutive modeling for two sands under high pressure." *Int. J. Geomech.* 21 (5): 04021042. https://doi.org/10.1061/(ASCE)GM.1943-5622.0001987.
Xiao, Y., J. Xiang, H. Liu, and Q. Ma. 2017b. "Strength-dilatancy relation of sand containing non-plastic fines." *Geotech. Lett.* 7 (2): 1–7. https://doi.org/http://dx.doi.org/10.1680/jgele.16.00144.
Xiao, Y., W. Xiao, H. Wu, Y. Liu, and H. Liu. 2023a. "Fracture of interparticle MICP bonds under compression." *Int. J. Geomech.* 23 (3): 04022316. https://doi.org/10.1061/IJGNAI.GMENG-8282.
Xiao, Y., Z. Yuan, J. Lin, J. Ran, B. Dai, J. Chu, and H. Liu. 2019c. "Effect of particle shape of glass beads on the strength and deformation of cemented sands." *Acta Geotech.* 14 (6): 2123–2131. https://doi.org/10.1007/s11440-019-00830-w.
Xiao, Y., X. Zhang, C. Wang, H. Cui, and H. Liu. 2023b. "Breakage-dependent fractional plasticity model for sands." *Int. J. Geomech.* 23 (3): 04022299. https://doi.org/10.1061/IJGNAI.GMENG-8140.
Xiao, Y., Z. Zhang, A. W. Stuedlein, and T. M. Evans. 2021b. "Liquefaction modeling for biocemented calcareous sand." *J. Geotech. Geoenviron. Eng.* 147 (12): 04021149. https://doi.org/10.1061/(ASCE)GT.1943-5606.0002666.
Yamamoto, Y., M. Hyodo, and R. P. Orense. 2009. "Liquefaction resistance of sandy soils under partially drained condition." *J. Geotech. Geoenviron. Eng.* 135 (8): 1032–1043. https://doi.org/10.1061/(ASCE)GT.1943-5606.0000051.
Yang, J., and X. D. Luo. 2015. "Exploring the relationship between critical state and particle shape for granular materials." *J. Mech. Phys. Solids* 84: 196–213. https://doi.org/10.1016/j.jmps.2015.08.001.

Yang, J., and X. D. Luo. 2018. "The critical state friction angle of granular materials: Does it depend on grading?" *Acta Geotech.* 13 (3): 535–547. https://doi.org/10.1007/s11440-017-0581-x.

Yang, J., and L. M. Wei. 2012. "Collapse of loose sand with the addition of fines: The role of particle shape." *Géotechnique* 62 (12): 1111–1125. https://doi.org/10.1680/geot.11.P.062.

Yang, S. L., R. Sandven, and L. Grande. 2006. "Steady-state lines of sand-silt mixtures." *Can. Geotech. J.* 43 (11): 1213–1219. https://doi.org/10.1139/t06-069.

Yao, Y.-P., H. Yamamoto, and N.-D. Wang. 2008. "Constitutive model considering sand crushing." *Soils Found.* 48 (4): 603–608. https://doi.org/10.3208/sandf.48.603.

Yilmaz, Y., Y. Deng, C. S. Chang, and A. Gokce. 2023. "Strength–dilatancy and critical state behaviours of binary mixtures of graded sands influenced by particle size ratio and fines content." *Géotechnique* 73 (3): 202–217. https://doi.org/10.1680/jgeot.20.P.320.

Yu, F. 2019. "Influence of particle breakage on behavior of coral sands in triaxial tests." *Int. J. Geomech.* 19 (12): 04019131. https://doi.org/10.1061/(asce)gm.1943-5622.0001524.

Zeybek, A., and S. P. G. Madabhushi. 2019. "Simplified procedure for prediction of earthquake-induced settlements in partially saturated soils." *J. Geotech. Geoenviron. Eng.* 145 (11): 04019100. https://doi.org/10.1061/(ASCE)GT.1943-5606.0002173.

Zhang, J., and M. Luo. 2020. "Dilatancy and critical state of calcareous sand incorporating particle breakage." *Int. J. Geomech.* 20 (4): 04020030. https://doi.org/10.1061/(ASCE)GM.1943-5622.0001637.

Zhang, J., S.-C. R. Lo, M. Rahman, and J. Yan. 2018. "Characterizing monotonic behavior of pond ash within critical state approach." *J. Geotech. Geoenviron. Eng.* 144 (1): 04017100. https://doi.org/10.1061/(ASCE)GT.1943-5606.0001798.

Zhang, Z.-T., W.-H. Gao, X. Wang, J.-Q. Zhang, and X.-Y. Tang. 2020. "Degradation-induced evolution of particle roundness and its effect on the shear behaviour of railway ballast." *Transp. Geotech.* 24: 100388. https://doi.org/10.1016/j.trgeo.2020.100388.

Zhao, S., and X. Zhou. 2017. "Effects of particle asphericity on the macro- and micro-mechanical behaviors of granular assemblies." *Granular Matter* 19 (2): 38. https://doi.org/10.1007/s10035-017-0725-6.

Zhou, Y., H. Wang, B. Zhou, and J. Li. 2018. "DEM-aided direct shear testing of granular sands incorporating realistic particle shape." *Granular Matter* 20 (3): 55. https://doi.org/10.1007/s10035-018-0828-8.